Molecular Thermodynamics of LNA:LNA Base Pairs and the Hyperstabilizing Effect of 5′-Proximal LNA:DNA Base Pairs

Kareem Fakhfakh
Michael Smith Laboratories, University of British Columbia, Vancouver, BC, Canada

Dept. of Chemical and Biological Engineering, University of British Columbia, Vancouver, BC, Canada

Olivia Marais, Xin Bo Justin Cheng, and Jorge Real Castañeda
Dept. of Chemical and Biological Engineering, University of British Columbia, Vancouver, BC, Canada

Curtis B. Hughesman
Michael Smith Laboratories, University of British Columbia, Vancouver, BC, Canada

Charles Haynes
Michael Smith Laboratories, University of British Columbia, Vancouver, BC, Canada

Dept. of Chemical and Biological Engineering, University of British Columbia, Vancouver, BC, Canada

RES'EAU Water Research Network, Dept. of Chemical and Biological Engineering, University of British Columbia, Vancouver, BC, Canada

DOI 10.1002/aic.14916
Published online August 7, 2015 in Wiley Online Library (wileyonlinelibrary.com)

Locked nucleic acids (LNAs) can greatly enhance duplex DNA stability, and are therefore creating opportunities to improve therapeutics, as well as PCR-based disease and pathogen diagnostics. Realizing the full potential of LNAs will require better understanding of their contributions to duplex stability, and the ability to predict their hydridization thermodynamics. Melting thermodynamics data for a large set of diverse duplexes containing LNAs in one or both strands are presented. Those data reveal that LNAs, when present on both strands, can stabilize a duplex not only through direct interaction with their base-pair partner, but also through nonlocal hyperstablization effects created by LNA:LNA base pairs and/or specific patterns of oppositely oriented LNA:DNA base pairs. The data are, therefore, used to extend a thermodynamic model previously developed in our lab to permit accurate prediction of melting temperatures for duplexes bearing LNA substitutions within both strands using a classic group-contribution approach. © 2015 American Institute of Chemical Engineers *AIChE J*, 61: 2711–2731, 2015
Keywords: oligonucleotide, locked nucleic acid, deoxyribonucleic acid, DNA stability, nearest neighbor thermodynamics, group-contribution model

Introduction

Significant advances in non-natural nucleotide chemistry have been made over the past quarter century, motivated in part by the desire to enhance diagnostic and therapeutic applications of structured oligonucleotides by improving their thermodynamic and chemical (e.g., nuclease-resistance) stability, or by altering their cellular uptake.[1] Among the most significant and widely used nucleotide modifications[2,3] is the locked nucleic acid (LNA),[4,5] in which a methylene bridge has been introduced between the 4′-carbon and 2′-oxygen of the ribose sugar to "lock" it in a C3′-*endo* (RNA-like) conformation.[6–8] Replacement of a DNA or RNA nucleotide with its corresponding LNA can increase the stability, and thus the melting temperature T_m, of a duplex. For duplex DNA (dsDNA), an LNA substitution in one strand generally increases T_m by 1–8°C, while somewhat larger increases in T_m (2–10°C) are observed when a DNA strand (ssDNA) containing a single LNA substitution is paired with its complementary RNA strand.[9,10]

LNA-containing oligonucleotides are finding increasing use as therapeutics, including as gene-silencing agents,[11,12] and as DNA or RNA aptamers.[13,14] The introduction of LNA monomers into a standard ssDNA or ssRNA aptamer can greatly improve both the thermodynamic and serum stability of the structured single-strand, without introducing immunogenicity or toxicity effects that could otherwise deter therapeutic use.[15] LNA-substituted oligonucleotides have also found widespread use in a range of diagnostic applications, including real-time PCR, digital PCR, and hybridization-array-based detection of either germline mutations (e.g., single nucleotide polymorphisms) or somatic mutations associated with disease,[16,17] as

Correspondence concerning this article should be addressed to C. Hughesman at curtish@msl.ubc.ca or C. Haynes at israels@chbe.ubc.ca.

well as detection of either viral or microbial pathogens within foods and drinking water sources.[18]

The growing importance of LNAs in oligonucleotide-based medicine and diagnostics has motivated careful analysis of the properties of LNA-containing ssDNA, ssRNA, dsDNA, and hybrid DNA:RNA duplexes relative to their corresponding isosequential LNA-free forms.[19–22] A number of chemical and structural factors have thereby been found to contribute to LNA-mediated enhancement of thermal stability. NMR studies show that substitution of an LNA monomer into complementary dsDNA induces the modifed base pair and base pairs proximal to it to shift toward an A-form helix; a shift in the deoxyribose sugars toward a C3′-*endo* conformation is also observed.[23] An LNA substitution within the ssDNA of a DNA:RNA hybrid duplex likewise shifts the sugar toward a C3′-*endo* conformation.[23,24] This conformational change has also been characterized using both resonance Raman spectroscopy[25] and transient absorption[26,27] to intensify certain base-stacking interactions that are important determinants of secondary structure of LNA-containing duplexes, leading, for example, to a tendency toward the more thermally stable A-form in AT-rich sequences. Motivated by these and other structural insights,[8,28,29] thermodynamicists have conducted extensive studies aimed at quantifying the enthalpic and entropic contributions to the enhanced thermal stability of an LNA:DNA or LNA:RNA base pair.[6,7,9,19,21,22,30] Those studies, which typically rely on interpretation of melting thermodynamics collected by either UV spectroscopy[6,7,9,19,21,22] or differential scanning calorimetry,[19,31] show that the change in melting temperature (ΔT_m) accompanying an LNA substitution is sequence dependent, with the dominant determinant of the degree of stabilization being the type of base substituted.[19,21]

But for short B-form dsDNA, perhaps the greatest insights into the effect of LNA substitutions on duplex stability come from efforts to treat melting thermodynamic data with classic group-contribution modeling approaches, which have previously been used to great effect by Prausnitz[32,33] and others[34,35] to model thermodynamic behavior in a variety of other important liquid mixtures. The most widely used group-contribution type models developed for predicting T_m and melting thermodynamics of unsubstituted and LNA-substituted dsDNA are collectively known as nearest-neighbor thermodynamic (NNT) models.[19,21,22,30] Differences between available NNT models exist when applied to unsubstituted dsDNA, but collectively they predict that dsDNA melting thermodynamics depend on duplex length, as well as on the sequence and the overall *g–c* base-pair content. They assume, in accordance with more advanced theories derived from statistical mechanics (e.g., the Poland–Sheraga potential[36,37] and advances made to it by Fisher[38] and others[39]), that the sequence dependence arises, at least in part, from the combined contribution of base-pairing and base-stacking interactions. Both interactions are short-range in nature, permitting their contribution to the melting enthalpy ΔH to be captured through a set of nearest-neighbor enthalpy parameters for all unique $N_{3'+m}N_{3'+(m+1)}/N_{5'+m}N_{5'+(m+1)}$ base-pair doublets (tandem base pairs) in the duplex, where $N_{3'+m}$ is the nucleotide at the $3' + m$ base position on the sense strand. The melting entropy (ΔS) is handled in an analogous manner by computing the combined contribution to ΔS of base-pair formation and base-stacking interactions, which are both orientationally (e.g., bases stack in plane) and spatially specific; ΔS is thus also computed as the frequency-weighted sum of nearest-neighbor contributions. NNT models provide very good predictions of T_m for dsDNA melting between about 45 and 65°C.[40] In addition, good prediction of T_m values and melting thermodynamics (ΔH and ΔS) for duplexes melting above 65°C may be achieved by introducing heat capacity effects into an NNT model,[41] which is consistent with experiment and theory showing that dsDNA melting involves a heat capacity change ΔC_p of about 42 ± 16 cal mol^{-1} K^{-1} per base pair.[42]

NNT models that do or do not include ΔC_p contributions have been extended to predict changes in dsDNA stability arising from LNA substitution(s), generally for the case where those substitutions occur within only one strand.[19,21,22] Here, we focus on models that explicitly include ΔC_p contributions. To fix ideas, consider a short pure-DNA duplex that melts at a temperature $T_{m,\mathrm{DNA}}$ with a melting enthalpy and entropy of ΔH_{DNA} and ΔS_{DNA}, respectively. Substitution of an LNA into the duplex results in an increase in melting temperature from $T_{m,\mathrm{DNA}}$ to $T_{m,\mathrm{LNA}}$. The melting enthalpy and entropy of the LNA-modified duplex are then given by

$$\begin{aligned}\Delta H_{\mathrm{LNA}}\left(T_{m,\mathrm{LNA}}\right) &= \Delta H_{\mathrm{DNA}}\left(T_{m,\mathrm{DNA}}\right)+\Delta C_p\left(T_{m,\mathrm{LNA}}-T_{m,\mathrm{DNA}}\right)\\ &\quad+\Delta\Delta H_{\mathrm{LNA}}\\ \Delta S_{\mathrm{LNA}}\left(T_{m,\mathrm{LNA}}\right) &= \Delta S_{\mathrm{DNA}}\left(T_{m,\mathrm{DNA}}\right)+\Delta C_p\ln\left(T_{m,\mathrm{LNA}}/T_{m,\mathrm{DNA}}\right)\\ &\quad+\Delta\Delta S_{\mathrm{LNA}}\end{aligned} \tag{1}$$

where $\Delta\Delta H_{\mathrm{LNA}}$ accounts for the incremental change in the melting enthalpy due to intrinsic changes in base-pair and proximal duplex structure/energetics (e.g., changes in base stacking) that arise as a result of the LNA substitution and the formation of an LNA:DNA base pair. Equation 1 predicts that changes in ΔH (and likewise ΔS) may arise not only through a nonzero $\Delta\Delta H_{\mathrm{LNA}}$ (or by analogy $\Delta\Delta S_{\mathrm{LNA}}$) value, but also simply due to the fact that ΔH and ΔS are temperature dependent. Indeed, our recently described NNT model for LNA-containing dsDNA,[19] which accounts for the temperature dependence of ΔH and ΔS through a nonzero ΔC_p, predicts that experimentally observed changes in ΔS accompanying LNA substitutions in one strand arise from both the temperature dependence of ΔS and a negative $\Delta\Delta S_{\mathrm{LNA}}$ value that reflects restrictions to ribose sugar flexibility imposed by the methylene bridge, including the associated increase in structural preorganization of the LNA-containing single strand. Corresponding changes in ΔH, however, are generally found to arise only from the temperature dependence of ΔH, as $\Delta\Delta H_{\mathrm{LNA}}$ values for dsDNA substituted with a single LNA are statistically insignificant.[19] This finding is not at odds with observed changes in structure arising from an LNA substitution; it simply indicates that structural changes induced by individual LNA substitutions (e.g., increased local A-form helix characteristics) result in a set of subprocesses (perturbation of hydrogen bond strengths, base stacking energies, etc.) that are enthalpically compensatory in nature, such that the total incremental enthalpy change, $\Delta\Delta H_{\mathrm{LNA}}$, is either very small or athermal.

As noted, current NNT models are designed to predict melting thermodynamics of complementary or mismatched duplexes bearing LNA substitutions in one strand.[19,21,22] They are not intended to be applied to duplexes containing LNA substitutions within both strands, including those that form LNA:LNA base pairs. Melting studies have shown that complementary duplexes containing LNA:LNA base pairs can be exceptionally stable—a completely LNA-substituted 9-mer

duplex has been shown to melt at a T_m more than 60°C higher than that of the corresponding isosequential pure-DNA duplex.[6] In principle, NNT models can be extended to permit their application to duplexes bearing LNA substitutions on both strands. However, at present, the impact on melting thermodynamics of introducing additional LNA substitutions in various positions of an opposing pure-DNA strand is not well understood. Here, we address this issue, as the ability to understand and predict the thermal stability of duplex DNA bearing LNA substitutions within both strands may serve to expand applications of LNA technology in important areas. For example, Wang et al.[43] have used LNA:LNA base pairing to improve the sensitivity and selectivity of molecular beacons, while Morandi et al.[44] have described the paired use of an LNA-substituted allele-specific primer and LNA-substituted beacon probe to detect cancer-related somatic point mutations, such as the BRAF *V600E* mutation associated with metastatic melanoma and colorectal cancer, with increased sensitivity and specificity. In addition, several groups have reported on the use of LNA:LNA base pairs to greatly improve the thermal and serum stability of DNA aptamers targeted for therapeutic use.[15,45,46]

With the ultimate aim of establishing a NNT model that can be applied to short dsDNA bearing any pattern of LNA substitutions in either or both strands, we report here melting thermodynamic data for an extensive library of complementary duplexes in which an LNA substitution is made in a pure DNA strand at different positions relative to one or more LNAs on the opposite strand. The data are used to define (1) the duplex stabilization thermodynamics of an LNA:LNA base pair relative to the LNA:DNA base pairs from which it is formed, and (2) the impact on duplex stability of an LNA substitution made in one strand at a nucleotide position proximal to an existing LNA in the opposing strand. Results are then used to extend our current NNT model[19] to permit accurate prediction of T_m and ΔT_m values for duplexes bearing LNA substitutions on both complementary strands.

Method

Materials

All pure DNA and LNA containing oligonucleotides were obtained from either Integrated DNA Technologies (Coralville, IA) or Exiqon (Vedbæk, Denmark). Each strand was resuspended in buffer containing 1 M NaCl, 10 mM Na_2HPO_4, and 1 mM Na_2EDTA at pH = 7.0, and then quantified by UV spectrophotometry (Cary 1E; Santa Clara, CA) at 80°C using extinction coefficients provided by the supplier.

Measurement of melting thermodynamics by UV spectroscopy

Helix-to-coil melting transition data were collected on a Cary 1E spectrophotometer equipped with a 12-cell Peltier temperature controller. All UV-monitored melt (UVM) experiments were conducted at 260 nm by scanning from 25 to 95°C at a scan rate of 0.5°C min^{-1} to obtain absorbance (A_{260}) vs. T profiles. Experimental melting transition profiles and regressed thermodynamic values were scan-rate independent at scan rates $\leq$ 0.6°C min^{-1}. A cuvette with a path length of 10 mm was loaded with duplex sample to a total strand concentration C_T of 5 or 7.5 μM and then sealed to prevent evaporation during heating. Buffer reference and duplex melting curves were collected in triplicate and collectively analyzed to obtain mean

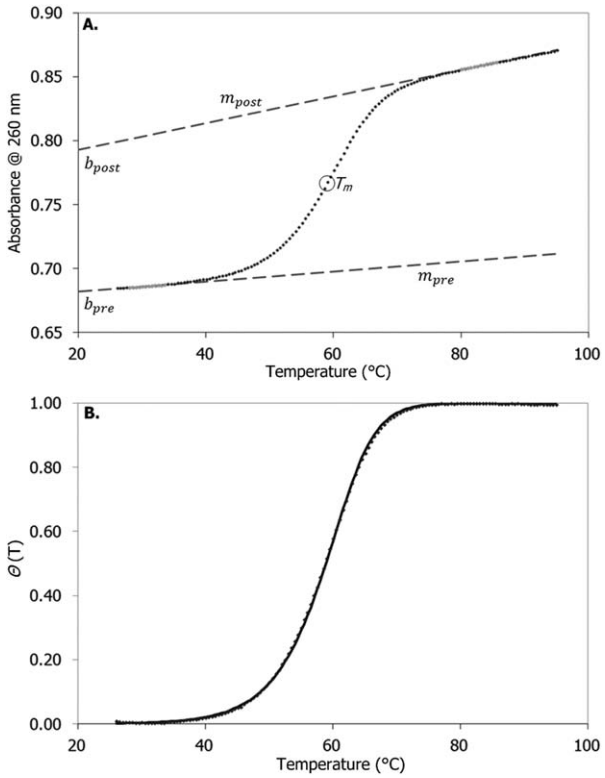

Figure 1. Melting transition measured by UV spectroscopy at 260 nm for the complementary duplex 5′-*ctaacgGatgc*−3′/5′-*gcatccgttag*−3′ at a total strand concentration C_T of 7.5 μM and in an aqueous buffer (pH 7.0) containing 1 M NaCl, 10 mM Na_2HPO_4, and 1 mM Na_2EDTA.

(A) Raw melting transition data; the slope (m) and intercept (b) of the pretransition (fully duplexed) and post-transition (fully dissociated) states are shown. (B) Pretransition and post-transition baseline normalized representation of the same melting transition data (diamonds), where θ is the fraction of strands in the single-stranded state; the two-state thermodynamic model fit (solid curve) is also shown and superimposes the experimental data.

values and standard deviations for T_m, $\Delta H(T_m)$, $\Delta S(T_m)$, and ΔG (at the reference temperature of 53°C), hereafter referred to as ΔG^o. Melting curve analysis followed a method we have previously described,[47] which assumes two-state melting thermodynamics and includes contributions from a nonzero ΔC_p. Briefly, from each buffer-scan-normalized melt curve, the fraction of strands in the random-coil state (θ) was determined as a function of temperature to create a fractional curve by fitting Eq. 2 to the pretransition and post-transition baselines

$$A_{260}(T) = \left(m_{\text{pre}}^{\text{UVM}}T + b_{\text{pre}}^{\text{UVM}}\right)(1-\theta) + \left(m_{\text{post}}^{\text{UVM}}T + b_{\text{post}}^{\text{UVM}}\right)\theta \quad (2)$$

where m_{pre} and b_{pre}, and m_{post} and b_{post} are the slopes and intercepts of the pretransition and post-transition baselines, respectively. A representative UVM experiment is provided in Figure 1A, within which are identified the slopes and intercepts of the two transition baselines used to normalize the melting transition data. Concordance between the normalized melting transition and two-state melting thermodynamics theory (Eq. 3 below) is also demonstrated (Figure 1B); for all

sequences studied, the experimental and two-state melting thermodynamics agree to within ±15%.

$\Delta H(T_m)$, $\Delta S(T_m)$, and T_m were determined by fitting Eqs. 3 and 4 to the resulting fractional curve

$$\theta(T) = \frac{-K_d(T) + \sqrt{K_d^2(T) + 2K_d(T)C_T}}{C_T} \tag{3}$$

$$K_d(T) = \exp\left[-\left(\frac{\Delta S + \Delta C_p(T - T_m)}{RT}\right) + \frac{\Delta S + \Delta C_p(T/T_m)}{R}\right] \tag{4}$$

where $K_d(T)$ is the temperature-dependent equilibrium constant for the melting reaction. The ΔC_p required in Eqs. 3 and 4 was computed as $\Delta C_p = n\Delta C_p^{bp}$, where n is the total number of base pairs in the duplex and ΔC_p^{bp} is the heat capacity change per base pair (bp), previously reported by Hughesman et al.[41] to be 42 cal mol^{-1} K^{-1} bp^{-1}. $T_{\max}$ was used as an estimate of T_m in Eq. 4 during the first solution iteration. After regressing values for $\Delta H(T_m)$ and $\Delta S(T_m)$, a new estimate of T_m for nonself-complementary duplexes was then obtained from

$$T_m = \frac{\Delta H(T_m)}{\Delta S(T_m) - R\ln(C_T/4)} \tag{5}$$

where C_T is the total strand concentration (M), and is divided by 4 when the two single strands are not self-complementary (C_T/4 is replaced by C_T when the two single strands are self-complementary. The model is otherwise the same). That iteration scheme was continued until a best fit was achieved.

Regression of model parameters

Levenberg–Marquardt (LM) type regression[48] to melting temperature (T_m) data was used to fit a set of parameters needed to compute the total hyperstabilization energy $\Delta\Delta G^{\circ}_{\text{hyper}}$ of a duplex that arises from (1) formation of an LNA:LNA base pair through replacement of a DNA nucleotide that is paired with an LNA within the complementary strand, and (2) substitution of an LNA into a pure-DNA strand at a position proximal to an oppositely oriented LNA:DNA base pair, or any combinations of those two substitution patterns. The parameters are used to extend our existing NNT model,[19] hereafter referred to as the standard single-base thermodynamic (standard SBT) model, that can be applied to duplexes containing LNA substitutions in one strand, but not both.

Regression of the resulting "extended SBT model" to the full dataset was conducted using MATLAB (R2007b) software. Based on an average experimental error σ_i in $\Delta\Delta T_m$ of ± 0.8°C, the regression scheme minimized the least squares of the residual (χ^2)

$$\chi^2 = \sum_i \left(\frac{\Delta\Delta T_{m\,(\text{expt})} - \Delta\Delta T_{m\,(\text{pred})}}{\sigma_i}\right)^2 \tag{6}$$

by initiating the objective function ($0 = \Delta\Delta T_{m\,(\text{expt})} - \Delta\Delta T_{m\,(\text{pred})}$) with a randomly generated set of parameter estimates. In Eq. 6, expt and pred indicate experimental and model predicted values, respectively, and $\Delta\Delta T_m$ is given by

$$\Delta\Delta T_m = \Delta T_{m,\text{LNA}} - \left(\Delta T_{m,\text{LNA:DNA}} + \Delta T_{m,\text{DNA:LNA}}\right) \tag{7}$$

where, for example

$$\Delta T_{m,\text{LNA}} = T_{m,\text{LNA}} - T_{m,\text{DNA}} \tag{8}$$

Here, subscript LNA specifies the duplex bearing an LNA substitution in each strand, and subscript DNA specifies the corresponding isosequential pure-DNA duplex. Subscript LNA:DNA specifies the same duplex when no LNA substitution has been made in the antisense-strand, and

$$\Delta T_{m,\text{LNA:DNA}} = T_{m,\text{LNA:DNA}} - T_{m,\text{DNA}} \tag{9}$$

In the extended SBT model, $T_{m,\text{LNA (pred)}}$ for a duplex bearing an LNA in each strand is given by

$$T_{m,\text{LNA (pred)}} = \frac{\Delta H_{\text{LNA}}\left(T_{m,\text{LNA (pred)}}\right) + \Delta\Delta G^{\circ}_{\text{hyper}}}{\Delta S_{\text{LNA}}\left(T_{m,\text{LNA (pred)}}\right) - R\ln\left(\frac{C_T}{4}\right)} \tag{10}$$

with ΔH_{LNA} and ΔS_{LNA} computed as

$$\Delta H_{\text{LNA}}\left(T_{m,\text{LNA}}\right) = \Delta H^{\circ}_{\text{DNA}} + \Delta C_p\left(T_{m,\text{LNA}} - T_{\text{ref}}\right) + \Delta\Delta H^{\circ}_{\text{LNA}} \tag{11}$$

and

$$\Delta S_{\text{LNA}}\left(T_{m,\text{LNA}}\right) = \Delta S^{\circ}_{\text{DNA}} + \Delta C_p \ln\left({}^{T_{m,\text{LNA}}}\!/_{T_{\text{ref}}}\right) + \Delta\Delta S^{\circ}_{\text{LNA}} \tag{12}$$

In both the standard ($\Delta\Delta G^{\circ}_{\text{hyper}} = 0$) and extended SBT models, the melting enthalpy $\Delta H^{\circ}_{\text{DNA}}$ and entropy $\Delta S^{\circ}_{\text{DNA}}$ for the isosequential pure-DNA duplex are computed at a specific reference (°) temperature (T_{ref}) of 53°C, from which their corresponding values at the T_m of the LNA substituted duplex can be computed using ΔC_p calculated as described above. A T_{ref} of 53°C is applied, as our previous work[41] showed that the NNT model (upon which the SBT model is based) predicts melting thermodynamics for pure-DNA duplexes with greatest accuracy when that reference temperature is applied. $\Delta\Delta H^{o}_{LNA}$ and $\Delta\Delta S^{o}_{LNA}$ represent the incremental change in the melting enthalpy and entropy, respectively, resulting from any pattern of LNA substitutions within one of the two strands; they are computed at T_{ref} from available standard SBT model parameters, and a comprehensive description of the original SBT model upon which the extended model (Eqs. 10–12) presented here is based can be found in our previous papers.[19,49] In Eq. 10, R is the ideal gas constant, 1.987 cal mol^{-1} K^{-1}.

The value of $\Delta\Delta G^{\circ}_{\text{hyper}}$, which represents the excess energetic contribution to duplex stability created by an LNA:LNA base pair and/or sets of proximal oppositely oriented LNA:DNA base pairs, is computed from the set of extended SBT model parameters $\Delta\Delta G^{o}_{\text{hyper}-(j)}$ as

$$\Delta\Delta G^{\circ}_{\text{hyper}} = \sum_j n_j \Delta\Delta G^{\circ}_{\text{hyper}-(j)} \tag{13}$$

In Eq. 13, n_j and $\Delta\Delta G^{o}_{\text{hyper}-(j)}$ then give the frequency (total representations) and energetic contribution to $\Delta\Delta G^{\circ}_{\text{hyper}}$, respectively, of each LNA:LNA base pair ($j = 0$) or set of proximal oppositely oriented LNA:DNA base pairs of type j. Here, j is an integer ranging from −4 to +3, and its value may be understood by considering the position of an LNA within the antisense strand of a duplex relative to a chosen LNA within the sense strand. To fix ideas, we show here by example how Eq. 13 is applied to a hypothetical duplex containing both

Table 1. Melting Thermodynamic Data Collected by UV Spectroscopy for a Library of Complementary Duplexes of Either Pure DNA or Bearing Different Patterns of LNA Substitutions on One Strand

Duplex Name	Sense Strand (5′–3′)	Antisense Strand (5′–3′)	Length (bp), Duplex Type	ΔH (kcal mol^{-1})	ΔS (cal mol^{-1} K^{-1})	$\Delta G°$ (kcal mol^{-1})	$\Delta\Delta G°$ (kcal mol^{-1})	T_m (°C)	ΔT_m (°C)
1[a]	*ttcatagccgt*	*acggctatgaa*	11	76.9 ± 1.0 (79.4)	209.1 ± 3.1 (216.6)	8.72 ± 0.05 (8.74)		53.8 ± 0.2 (53.8)	
1-S-L3:AS	*ttCatagccgt*	*acggctatgaa*	LNA:DNA	80.8 ± 0.9 (81.7)	217.6 ± 2.7 (219.8)	9.83 ± 0.04 (9.94)	1.10 ± 0.06	58.3 ± 0.1 (58.8)	4.6 ± 0.2
1-S-L4:AS	*ttcAtagccgt*	*acggctatgaa*	LNA:DNA	77.5 ± 1.2 (80.5)	209.2 ± 3.5 (218.2)	9.25 ± 0.03 (9.35)	0.52 ± 0.06	56.0 ± 0.1 (56.3)	2.2 ± 0.3
1-S-L5:AS	*ttcaTagccgt*	*acggctatgaa*	LNA:DNA	79.5 ± 2.5 (81.1)	213.8 ± 7.3 (219.1)	9.74 ± 0.06 (9.67)	1.01 ± 0.08	58.0 ± 0.1 (57.6)	4.3 ± 0.2
1-S-L6:AS	*ttcatAgccgt*	*acggctatgaa*	LNA:DNA	77.9 ± 0.7 (80.5)	210.0 ± 2.2 (218.2)	9.40 ± 0.05 (9.35)	0.67 ± 0.07	56.6 ± 0.2 (56.3)	2.9 ± 0.3
1-S-L7:AS	*ttcataGccgt*	*acggctatgaa*	LNA:DNA	78.1 ± 2.0 (81.0)	210.9 ± 6.1 (219.0)	9.29 ± 0.03 (9.61)	0.57 ± 0.06	56.2 ± 0.1 (57.4)	2.4 ± 0.2
1-S-L8:AS	*ttcatagCcgt*	*acggctatgaa*	LNA:DNA	80.5 ± 1.8 (81.7)	216.4 ± 5.4 (219.8)	9.93 ± 0.04 (9.94)	1.20 ± 0.06	58.8 ± 0.2 (58.8)	5.0 ± 0.3
1-S:AS-L9	*ttcatagccgt*	*acggctatGaa*	DNA:LNA	76.5 ± 2.6 (81.0)	207.2 ± 8.0 (219.0)	8.92 ± 0.07 (9.61)	0.20 ± 0.09	54.6 ± 0.3 (57.4)	0.8 ± 0.3
1-S:AS-L8	*ttcatagccgt*	*acggctaTgaa*	DNA:LNA	79.3 ± 2.0 (81.1)	214.2 ± 6.1 (219.1)	9.40 ± 0.05 (9.67)	0.68 ± 0.07	56.6 ± 0.1 (57.6)	2.8 ± 0.3
1-S:AS-L7	*ttcatagccgt*	*acggctAtgaa*	DNA:LNA	77.9 ± 1.8 (80.5)	210.9 ± 5.6 (218.2)	9.12 ± 0.03 (9.35)	0.39 ± 0.06	55.4 ± 0.1 (56.3)	1.7 ± 0.3
1-S:AS-L6	*ttcatagccgt*	*acggcTatgaa*	DNA:LNA	77.8 ± 0.9 (81.1)	205.7 ± 3.4 (219.1)	10.68 ± 0.01 (9.67)	1.96 ± 0.05	58.5 ± 0.1 (57.6)	4.8 ± 0.3
1-S:AS-L5	*ttcatagccgt*	*acggCtatgaa*	DNA:LNA	85.2 ± 0.9 (81.7)	228.9 ± 2.6 (219.8)	10.48 ± 0.07 (9.94)	1.75 ± 0.09	60.7 ± 0.3 (58.8)	7.0 ± 0.3
1-S:AS-L4	*ttcatagccgt*	*acgGctatgaa*	DNA:LNA	78.2 ± 0.6 (81.0)	210.2 ± 1.7 (219.0)	9.65 ± 0.03 (9.61)	0.92 ± 0.06	57.7 ± 0.1 (57.4)	4.0 ± 0.2
2[b]	*tgcggataagt*	*acttatccgca*	11	82.4 ± 2.3 (79.4)	225.6 ± 6.8 (216.6)	8.76 ± 0.03 (8.74)		53.8 ± 0.1 (53.8)	
2-S-L7:AS	*tgcggaTaagt*	*acttatccgca*	LNA:DNA	76.9 ± 4.4 (81.1)	207.0 ± 13.2 (219.1)	9.38 ± 0.13 (9.67)	0.62 ± 0.13	56.6 ± 0.3 (57.6)	2.8 ± 0.4
2-S:AS-L3	*tgcggataagt*	*acTtatccgca*	DNA:LNA	78.6 ± 4.6 (81.1)	212.5 ± 13.6 (219.1)	9.34 ± 0.14 (9.67)	0.58 ± 0.14	56.3 ± 0.4 (57.6)	2.5 ± 0.4
2-S-L7:AS	*tgcggataAgt*	*acttatccgca*	LNA:DNA	84.3 ± 0.7 (80.5)	228.4 ± 2.1 (218.2)	9.81 ± 0.02 (9.35)	1.05 ± 0.04	58.0 ± 0.0 (56.3)	4.2 ± 0.1
2-S:AS-L5	*tgcggataagt*	*acttAtccgca*	DNA:LNA	77.3 ± 0.4 (80.5)	209.2 ± 1.2 (218.2)	9.05 ± 0.02 (9.35)	0.29 ± 0.04	55.2 ± 0.1 (56.3)	1.3 ± 0.1
3[a]	*ctaacggatgc*	*gcatccgttag*	11	77.8 ± 1.7 (83.6)	211.8 ± 5.0 (229.7)	8.75 ± 0.04 (8.64)		53.9 ± 0.2 (53.4)	
3-S-L4:AS	*ctaAcggatgc*	*gcatccgttag*	LNA:DNA	77.5 ± 2.0 (84.7)	209.0 ± 5.8 (231.2)	9.35 ± 0.10 (9.25)	0.60 ± 0.10	56.4 ± 0.3 (55.8)	2.6 ± 0.4
3-S-L5:AS	*ctaaCggatgc*	*gcatccgttag*	LNA:DNA	80.1 ± 3.0 (85.7)	215.9 ± 8.9 (232.7)	9.70 ± 0.09 (9.84)	0.95 ± 0.10	57.8 ± 0.2 (58.1)	4.0 ± 0.2
3-S-L6:AS	*ctaacGgatgc*	*gcatccgttag*	LNA:DNA	79.3 ± 0.6 (85.1)	213.7 ± 1.8 (231.9)	9.62 ± 0.04 (9.51)	0.87 ± 0.06	57.5 ± 0.1 (56.8)	3.7 ± 0.2
3-S-L7:AS	*ctaacgGatgc*	*gcatccgttag*	LNA:DNA	80.6 ± 1.0 (85.1)	216.6 ± 2.8 (231.9)	9.97 ± 0.04 (9.51)	1.22 ± 0.06	59.0 ± 0.1 (56.8)	5.1 ± 0.2
3-S-L8:AS	*ctaacggAtgc*	*gcatccgttag*	LNA:DNA	77.4 ± 0.2 (84.7)	208.2 ± 0.8 (231.2)	9.45 ± 0.04 (9.25)	0.70 ± 0.05	56.9 ± 0.2 (55.8)	3.1 ± 0.2

TABLE 1. *Continued*

Duplex Name	Sense Strand (5′–3′)	Antisense Strand (5′–3′)	Length (bp), Duplex Type	ΔH (kcal mol^{-1})	ΔS (cal mol^{-1} K^{-1})	$\Delta G°$ (kcal mol^{-1})	$\Delta\Delta G°$ (kcal mol^{-1})	T_m (°C)	ΔT_m (°C)
3-S:AS-L9	*ctaacggatgc*	*gcatccgtTag*	DNA:LNA	85.3 ± 1.1 (85.2)	232.2 ± 3.4 (232.0)	9.58 ± 0.02 (9.57)	0.83 ± 0.04	57.0 ± 0.0 (57.0)	3.2 ± 0.2
3-S:AS-L8	*ctaacggatgc*	*gcatccgTtag*	DNA:LNA	77.2 ± 1.3 (85.2)	207.4 ± 3.9 (232.0)	9.52 ± 0.02 (9.57)	0.77 ± 0.05	57.2 ± 0.1 (57.0)	3.4 ± 0.2
3-S:AS-L7	*ctaacggatgc*	*gcatccGttag*	DNA:LNA	79.8 ± 0.8 (85.1)	215.1 ± 2.4 (231.9)	9.66 ± 0.04 (9.51)	0.91 ± 0.06	57.7 ± 0.1 (56.8)	3.8 ± 0.2
3-S:AS-L6	*ctaacggatgc*	*gcatcCgttag*	DNA:LNA	79.8 ± 1.3 (85.7)	213.9 ± 3.9 (232.7)	9.99 ± 0.07 (9.84)	1.24 ± 0.08	59.1 ± 0.2 (58.1)	5.3 ± 0.3
3-S:AS-L5	*ctaacggatgc*	*gcatCcgttag*	DNA:LNA	79.8 ± 0.7 (85.7)	214.2 ± 2.1 (232.7)	9.95 ± 0.07 (9.84)	1.21 ± 0.08	59.0 ± 0.3 (58.1)	5.1 ± 0.3
3-S:AS-L4	*ctaacggatgc*	*gcaTccgttag*	DNA:LNA	77.3 ± 1.5 (85.2)	207.5 ± 4.4 (232.0)	9.57 ± 0.04 (9.57)	0.82 ± 0.05	57.4 ± 0.1 (57.0)	3.6 ± 0.2
4[a]	*ctacgcattcc*	*ggaatgcgtag*	11	78.5 ± 2.6 (83.6)	214.0 ± 7.7 (229.7)	8.65 ± 0.06 (8.64)		53.4 ± 0.3 (53.4)	
4-S-L9:AS	*ctacgcatTcc*	*ggaatgcgtag*	LNA:DNA	79.6 ± 1.5 (85.2)	214.4 ± 4.2 (232.0)	9.69 ± 0.06 (9.57)	1.04 ± 0.09	57.8 ± 0.2 (57.0)	4.4 ± 0.3
4-S-L8:AS	*ctacgcaTtcc*	*ggaatgcgtag*	LNA:DNA	76.3 ± 0.2 (85.2)	205.0 ± 0.5 (232.0)	9.40 ± 0.01 (9.57)	0.75 ± 0.07	56.7 ± 0.1 (57.0)	3.3 ± 0.3
4-S-L7:AS	*ctacgcAttcc*	*ggaatgcgtag*	LNA:DNA	72.8 ± 1.7 (84.7)	195.6 ± 5.0 (231.2)	9.02 ± 0.06 (9.25)	0.37 ± 0.08	55.2 ± 0.2 (55.8)	1.7 ± 0.3
4-S-L6:AS	*ctacgCattcc*	*ggaatgcgtag*	LNA:DNA	82.0 ± 2.4 (85.7)	220.0 ± 7.2 (232.7)	10.23 ± 0.09 (9.84)	1.57 ± 0.11	60.0 ± 0.2 (58.1)	6.5 ± 0.3
4-S-L4:AS	*ctaCgcattcc*	*ggaatgcgtag*	LNA:DNA	79.4 ± 3.1 (85.7)	213.4 ± 9.3 (232.7)	9.75 ± 0.10 (9.84)	1.10 ± 0.12	58.1 ± 0.2 (58.1)	4.7 ± 0.3
4-S:AS-L3	*ctacgcattcc*	*ggAatgcgtag*	DNA:LNA	79.8 ± 3.1 (84.7)	216.1 ± 9.2 (231.2)	9.35 ± 0.08 (9.25)	0.69 ± 0.10	56.3 ± 0.2 (55.8)	2.9 ± 0.3
4-S:AS-L5	*ctacgcattcc*	*ggaaTgcgtag*	DNA:LNA	82.1 ± 0.4 (85.2)	222.0 ± 1.2 (232.0)	9.66 ± 0.02 (9.57)	1.00 ± 0.07	57.5 ± 0.1 (57.0)	4.1 ± 0.3
4-S:AS-L6	*ctacgcattcc*	*ggaatGcgtag*	DNA:LNA	78.2 ± 2.1 (85.1)	211.6 ± 6.4 (231.9)	9.14 ± 0.06 (9.51)	0.48 ± 0.09	55.5 ± 0.2 (56.8)	2.1 ± 0.3
4-S:AS-L8	*ctacgcattcc*	*ggaatgcGtag*	DNA:LNA	81.3 ± 3.4 (85.1)	220.9 ± 10.5 (231.9)	9.30 ± 0.10 (9.51)	0.65 ± 0.12	56.1 ± 0.4 (56.8)	2.6 ± 0.4
5[b]	*ctattggcgac*	*gtcgccaatag*	11	82.4 ± 1.5 (83.6)	224.3 ± 4.4 (229.7)	9.24 ± 0.05 (8.64)		55.8 ± 0.1 (53.4)	
5-S-L8:AS	*ctattggCgac*	*gtcgccaatag*	LNA:DNA	79.1 ± 1.9 (85.7)	211.0 ± 5.9 (232.7)	10.21 ± 0.06 (9.84)	0.97 ± 0.08	60.2 ± 0.3 (58.1)	4.4 ± 0.3
5-S:AS-L6	*ctattggcgac*	*gtcgcCaatag*	DNA:LNA	81.9 ± 1.6 (85.7)	219.9 ± 4.6 (232.7)	10.11 ± 0.06 (9.84)	0.87 ± 0.07	59.5 ± 0.1 (58.1)	3.7 ± 0.2
6	*ctgaagtccgc*	*gcggacttcag*	11	82.7 ± 2.8 (87.1)	223.3 ± 8.5 (237.2)	9.80 ± 0.10 (9.75)		58.1 ± 0.2 (57.6)	
6-S-L3:AS	*ctGaagtccgc*	*gcggacttcag*	LNA:DNA	90.2 ± 1.3 (88.7)	245.2 ± 3.7 (239.2)	10.19 ± 0.05 (10.62)	0.39 ± 0.11	59.2 ± 0.1 (61.0)	1.1 ± 0.2
6-S-L4:AS	*ctgAagtccgc*	*gcggacttcag*	LNA:DNA	96.2 ± 1.1 (88.2)	260.2 ± 3.2 (238.6)	11.26 ± 0.04 (10.36)	1.46 ± 0.11	62.7 ± 0.1 (60.0)	4.6 ± 0.2
6-S-L5:AS	*ctgaAgtccgc*	*gcggacttcag*	LNA:DNA	91.3 ± 1.3 (88.2)	244.8 ± 3.7 (238.6)	11.38 ± 0.07 (10.36)	1.58 ± 0.13	63.8 ± 0.2 (60.0)	5.7 ± 0.3
6-S-L6:AS	*ctgaaGtccgc*	*gcggacttcag*	LNA:DNA	91.0 ± 1.3 (88.7)	244.9 ± 3.7 (239.2)	11.05 ± 0.06 (10.62)	1.25 ± 0.12	62.5 ± 0.1 (61.0)	4.4 ± 0.2
6-S:AS-L3	*ctgaagtccgc*	*gcGgacttcag*	DNA:LNA	90.5 ± 1.3 (88.7)	245.1 ± 3.7 (239.2)	10.55 ± 0.04 (10.62)	0.76 ± 0.11	60.6 ± 0.1 (61.0)	2.5 ± 0.2

TABLE 1. *Continued*

Duplex Name	Sense Strand (5′–3′)	Antisense Strand (5′–3′)	Length (bp), Duplex Type	ΔH (kcal mol^{-1})	ΔS (cal mol^{-1} K^{-1})	$\Delta G°$ (kcal mol^{-1})	$\Delta\Delta G°$ (kcal mol^{-1})	T_m (°C)	ΔT_m (°C)
6-S:AS-L4	*ctgaagtccgc*	*gcgGacttcag*	DNA:LNA	91.1 ± 1.3 (88.7)	244.9 ± 3.7 (239.2)	11.13 ± 0.07 (10.62)	1.33 ± 0.13	62.8 ± 0.1 (61.0)	4.7 ± 0.2
6-S:AS-L5	*ctgaagtccgc*	*gcggActtcag*	DNA:LNA	91.1 ± 1.3 (88.2)	244.9 ± 3.7 (238.6)	11.14 ± 0.06 (10.36)	1.34 ± 0.12	62.8 ± 0.1 (60.0)	4.7 ± 0.2
6-S:AS-L6	*ctgaagtccgc*	*gcggaCttcag*	DNA:LNA	91.5 ± 1.3 (89.3)	244.7 ± 3.7 (240.0)	11.63 ± 0.07 (10.95)	1.83 ± 0.12	64.7 ± 0.2 (62.3)	6.6 ± 0.3
7	*gtatcaagtct*	*agacttgatac*	11	77.5 ± 2.5 (73.4)	215.6 ± 7.8 (204.7)	7.15 ± 0.03 (6.61)		47.3 ± 0.2 (44.8)	
7-S:AS-L5	*gtatcaagtct*	*agacTtgatac*	DNA:LNA	80.9 ± 1.3 (75.2)	223.7 ± 4.0 (207.5)	7.90 ± 0.02 (7.54)	0.76 ± 0.04	50.5 ± 0.1 (48.8)	3.2 ± 0.3
7-S:AS-L6	*gtatcaagtct*	*agactTgatac*	DNA:LNA	83.4 ± 0.5 (75.2)	230.7 ± 1.7 (207.5)	8.12 ± 0.00 (7.54)	0.97 ± 0.03	51.3 ± 0.0 (48.8)	4.0 ± 0.2
7-S:AS-L4	*gtatcaagtct*	*agaCttgatac*	DNA:LNA	77.6 ± 1.1 (75.8)	211.4 ± 3.2 (208.3)	8.67 ± 0.02 (7.81)	1.53 ± 0.03	53.5 ± 0.1 (49.9)	6.2 ± 0.3
7-S-L3:AS	*gtAtcaagtct*	*agacttgatac*	LNA:DNA	83.6 ± 0.6 (74.6)	232.5 ± 1.7 (206.6)	7.73 ± 0.01 (7.22)	0.58 ± 0.03	49.9 ± 0.1 (47.4)	2.6 ± 0.2
7-S-L4:AS	*gtaTcaagtct*	*agacttgatac*	LNA:DNA	80.9 ± 1.3 (75.2)	223.7 ± 4.0 (207.5)	7.90 ± 0.02 (7.54)	0.76 ± 0.04	50.5 ± 0.1 (48.8)	3.2 ± 0.3
7-S-L5:AS	*gtatCaagtct*	*agacttgatac*	LNA:DNA	81.5 ± 4.1 (75.8)	224.7 ± 12.3 (208.3)	8.27 ± 0.07 (7.81)	1.12 ± 0.08	51.9 ± 0.3 (49.9)	4.6 ± 0.4
7-S-L6:AS	*gtatcAagtct*	*agacttgatac*	LNA:DNA	82.6 ± 2.1 (74.6)	229.8 ± 6.5 (206.6)	7.69 ± 0.00 (7.22)	0.54 ± 0.03	49.7 ± 0.1 (47.4)	2.4 ± 0.3
8[c]	*ggacctcgac*	*gtcgaggtcc*	10	78.1 ± 3.0 (75.5)	212.2 ± 9.2 (204.7)	8.85 ± 0.17 (8.76)		53.2 ± 0.8 (52.8)	
8-S-L4:AS[c]	*ggaCctcgac*	*gtcgaggtcc*	LNA:DNA	81.2 ± 4.0 (77.7)	217.0 ± 11.9 (207.6)	10.44 ± 0.11 (9.96)	1.59 ± 0.21	59.8 ± 0.2 (58.0)	6.6 ± 0.8
8-S-L5:AS[c]	*ggacCtcgac*	*gtcgaggtcc*	LNA:DNA	79.9 ± 2.2 (77.7)	214.4 ± 6.7 (207.6)	9.93 ± 0.12 (9.96)	1.09 ± 0.21	57.7 ± 0.5 (58.0)	4.5 ± 0.9
8-S-L7:AS[c]	*ggacctCgac*	*gtcgaggtcc*	LNA:DNA	88.7 ± 1.8 (77.7)	240.9 ± 5.2 (207.6)	10.08 ± 0.09 (9.96)	1.23 ± 0.20	57.8 ± 0.3 (58.0)	4.6 ± 0.8
8-S:AS-L5	*ggacctcgac*	*gtcgAggtcc*	DNA:LNA	82.2 ± 2.1 (76.6)	220.0 ± 6.3 (206.2)	10.41 ± 0.09 (9.37)	1.57 ± 0.20	59.6 ± 0.3 (55.4)	6.4 ± 0.8
8-S:AS-L6	*ggacctcgac*	*gtcgaGgtcc*	DNA:LNA	79.7 ± 1.7 (77.1)	212.1 ± 5.3 (206.8)	10.50 ± 0.06 (9.63)	1.65 ± 0.18	60.2 ± 0.3 (56.6)	7.0 ± 0.8
8-S:AS-L7	*ggacctcgac*	*gtcgagGtcc*	DNA:LNA	77.9 ± 2.2 (77.1)	208.4 ± 6.5 (206.8)	9.95 ± 0.07 (9.63)	1.10 ± 0.19	57.9 ± 0.2 (56.6)	4.7 ± 0.8
8-S:AS-L67	*ggacctcgac*	*gtcgaGGtcc*	Tandem	83.7 ± 0.9 (78.7)	221.7 ± 2.4 (208.9)	11.37 ± 0.12 (10.5)	2.53 ± 0.21	63.6 ± 0.5 (60.3)	10.4 ± 0.9
8-S-L45:AS	*ggaCCtcgac*	*gtcgaggtcc*	Tandem	80.5 ± 3.8 (79.9)	213.3 ± 10.9 (210.5)	10.92 ± 0.22 (11.15)	2.07 ± 0.28	62.0 ± 0.5 (63.2)	8.8 ± 0.9
8-S-L57:AS	*ggacCtCgac*	*gtcgaggtcc*	Gapmer	83.0 ± 1.5 (79.9)	219.4 ± 4.4 (210.5)	11.36 ± 0.09 (11.15)	2.51 ± 0.20	63.6 ± 0.2 (63.2)	10.5 ± 0.8
9	*cctgcgatgac*	*gtcatcgcagg*	11	86.2 ± 3.8 (86.7)	233.9 ± 11.4 (235.9)	9.89 ± 0.09 (9.78)		57.4 ± 0.2 (56.7)	
9-S-L3:AS	*ccTgcgatgac*	*gtcatcgcagg*	LNA:DNA	92.4 ± 0.8 (88.4)	249.9 ± 2.3 (238.0)	10.88 ± 0.03 (10.71)	0.99 ± 0.10	60.6 ± 0.1 (60.3)	3.2 ± 0.2
9-S-L4:AS	*cctGcgatgac*	*gtcatcgcagg*	LNA:DNA	86.8 ± 3.8 (88.3)	234.7 ± 11.3 (237.9)	10.26 ± 0.08 (10.66)	0.37 ± 0.12	58.6 ± 0.1 (60.1)	1.2 ± 0.2
9-S-L5:AS	*cctgCgatgac*	*gtcatcgcagg*	LNA:DNA	87.6 ± 3.8 (88.9)	234.4 ± 11.3 (238.6)	11.13 ± 0.09 (10.98)	1.24 ± 0.13	62.1 ± 0.1 (61.4)	4.7 ± 0.2

TABLE 1. *Continued*

Duplex Name	Sense Strand (5′–3′)	Antisense Strand (5′–3′)	Length (bp), Duplex Type	ΔH (kcal mol^{-1})	ΔS (cal mol^{-1} K^{-1})	$\Delta G°$ (kcal mol^{-1})	$\Delta\Delta G°$ (kcal mol^{-1})	T_m (°C)	ΔT_m (°C)
9-S-L6:AS	*cctgcGatgac*	*gtcatcgcagg*	LNA:DNA	87.1 ± 3.8 (88.3)	234.6 ± 11.3 (237.9)	10.59 ± 0.09 (10.66)	0.70 ± 0.13	59.9 ± 0.0 (60.1)	2.5 ± 0.2
9-S-L7:AS	*cctgcgAtgac*	*gtcatcgcagg*	LNA:DNA	87.2 ± 3.8 (87.8)	234.6 ± 11.3 (237.3)	10.65 ± 0.15 (10.39)	0.76 ± 0.18	60.2 ± 0.3 (59.1)	2.8 ± 0.4
9-S-L8:AS	*cctgcgaTgac*	*gtcatcgcagg*	LNA:DNA	87.5 ± 3.8 (88.4)	234.5 ± 11.3 (238.0)	11.00 ± 0.15 (10.71)	1.11 ± 0.17	61.6 ± 0.2 (60.3)	4.2 ± 0.3
9-S:AS-L3	*cctgcgatgac*	*gtCatcgcagg*	DNA:LNA	87.7 ± 3.8 (88.9)	234.4 ± 11.3 (238.6)	11.14 ± 0.11 (10.98)	1.25 ± 0.15	62.1 ± 0.1 (61.4)	4.7 ± 0.3
9-S:AS-L4	*cctgcgatgac*	*gtcAtcgcagg*	DNA:LNA	90.7 ± 2.8 (87.8)	246.2 ± 8.4 (237.3)	10.38 ± 0.10 (10.39)	0.48 ± 0.14	58.8 ± 0.2 (59.1)	1.4 ± 0.3
9-S:AS-L5	*cctgcgatgac*	*gtcaTcgcagg*	DNA:LNA	87.4 ± 3.8 (88.4)	234.5 ± 11.3 (238.0)	10.89 ± 0.06 (10.71)	1.00 ± 0.11	61.1 ± 0.1 (60.3)	3.7 ± 0.3
9-S:AS-L6	*cctgcgatgac*	*gtcatCgcagg*	DNA:LNA	94.6 ± 1.8 (88.9)	255.3 ± 5.3 (238.6)	11.26 ± 0.06 (10.98)	1.37 ± 0.11	61.9 ± 0.0 (61.4)	4.5 ± 0.2
9-S:AS-L7	*cctgcgatgac*	*gtcatcGcagg*	DNA:LNA	86.9 ± 3.8 (88.3)	234.7 ± 11.3 (237.9)	10.29 ± 0.08 (10.66)	0.40 ± 0.12	58.7 ± 0.1 (60.1)	1.3 ± 0.2
10[c]	*ggaacaagatgc*	*gcatcttgttcc*	12	88.4 ± 3.4 (91.2)	242.7 ± 10.4 (251.0)	9.23 ± 0.12 (9.38)		54.6 ± 0.5 (55.1)	
10-S-L4:AS	*ggaAcaagatgc*	*gcatcttgttcc*	LNA:DNA	87.5 ± 2.2 (92.3)	238.6 ± 6.6 (252.5)	9.68 ± 0.06 (9.99)	0.45 ± 0.13	56.3 ± 0.2 (57.3)	1.7 ± 0.5
10-S-L6:AS[c]	*ggaacAagatgc*	*gcatcttgttcc*	LNA:DNA	89.0 ± 1.9 (92.3)	243.3 ± 5.8 (252.5)	9.62 ± 0.06 (9.99)	0.39 ± 0.13	56.0 ± 0.2 (57.3)	1.4 ± 0.5
10-S-L7:AS[c]	*ggaacaAgatgc*	*gcatcttgttcc*	LNA:DNA	94.4 ± 3.5 (92.3)	258.1 ± 10.5 (252.5)	10.24 ± 0.09 (9.99)	1.01 ± 0.15	58.2 ± 0.2 (57.3)	3.5 ± 0.5
10-S-L9:AS[c]	*ggaacaagAtgc*	*gcatcttgttcc*	LNA:DNA	91.8 ± 2.0 (92.3)	251.0 ± 6.1 (252.5)	9.96 ± 0.08 (9.99)	0.73 ± 0.14	57.3 ± 0.2 (57.3)	2.6 ± 0.5
10-S:AS-L5	*ggaacaagatgc*	*gcatCttgttcc*	DNA:LNA	93.6 ± 2.5 (93.4)	254.3 ± 7.3 (253.9)	10.62 ± 0.10 (10.58)	1.39 ± 0.15	59.6 ± 0.2 (59.4)	5.0 ± 0.5
10-S:AS-L6	*ggaacaagatgc*	*gcatcTtgttcc*	DNA:LNA	91.3 ± 1.5 (92.9)	249.5 ± 4.4 (253.3)	9.96 ± 0.05 (10.30)	0.73 ± 0.13	57.2 ± 0.1 (58.4)	2.6 ± 0.5
10-S:AS-L7	*ggaacaagatgc*	*gcatctTgttcc*	DNA:LNA	89.1 ± 1.5 (92.9)	241.3 ± 4.5 (253.3)	10.37 ± 0.05 (10.30)	1.14 ± 0.13	58.9 ± 0.1 (58.4)	4.3 ± 0.5
10-S:AS-L8	*ggaacaagatgc*	*gcatcttGttcc*	DNA:LNA	98.5 ± 1.9 (92.8)	270.3 ± 5.6 (253.1)	10.33 ± 0.04 (10.25)	1.10 ± 0.12	58.2 ± 0.1 (58.2)	3.6 ± 0.5
10-S-L46:AS	*ggaAcAagatgc*	*gcatcttgttcc*	Gapmer	92.3 ± 1.8 (93.5)	249.9 ± 5.3 (254.0)	10.75 ± 0.08 (10.60)	1.52 ± 0.14	60.1 ± 0.2 (59.5)	5.6 ± 0.5
10-S-L67:AS	*ggaacAAgatgc*	*gcatcttgttcc*	Tandem	90.8 ± 0.5 (93.5)	246.1 ± 1.5 (254.0)	10.53 ± 0.01 (10.60)	1.30 ± 0.12	59.4 ± 0.0 (59.5)	4.9 ± 0.5
10-S-L79:AS	*ggaacaAgAtgc*	*gcatcttgttcc*	Gapmer	93.3 ± 0.9 (93.5)	251.8 ± 2.5 (254.0)	11.10 ± 0.06 (10.60)	1.87 ± 0.13	61.4 ± 0.2 (59.5)	6.8 ± 0.5
10-S:AS-L67	*ggaacaagatgc*	*gcatcTTgttcc*	Tandem	89.8 ± 2.2 (94.6)	241.4 ± 6.3 (255.5)	11.05 ± 0.12 (11.23)	1.82 ± 0.17	61.6 ± 0.3 (61.8)	7.0 ± 0.5
11	*acgaccagagttacag*	*ctgtaactctggtcgt*	16	117.2 ± 2.4 (130.3)	317.3 ± 6.9 (357.4)	13.54 ± 0.11 (13.61)		67.3 ± 0.0 (65.8)	
11-S:AS-L4	*acgaccagagttacag*	*ctgTaactctggtcgt*	DNA:LNA	122.2 ± 1.9 (132.0)	329.1 ± 5.5 (359.5)	14.60 ± 0.11 (14.55)	1.06 ± 0.15	70.1 ± 0.1 (68.3)	2.7 ± 0.1
11-S:AS-L5	*acgaccagagttacag*	*ctgtAactctggtcgt*	DNA:LNA	120.0 ± 0.7 (131.4)	324.2 ± 2.1 (358.8)	14.05 ± 0.02 (14.23)	0.52 ± 0.11	68.6 ± 0.1 (67.4)	1.3 ± 0.1
11-S:AS-L6	*acgaccagagttacag*	*ctgtaActctggtcgt*	DNA:LNA	113.7 ± 1.1 (131.4)	304.4 ± 3.3 (358.8)	14.08 ± 0.05 (14.23)	0.55 ± 0.12	69.8 ± 0.0 (67.4)	2.4 ± 0.1

TABLE 1. *Continued*

Duplex Name	Sense Strand (5′–3′)	Antisense Strand (5′–3′)	Length (bp), Duplex Type	ΔH (kcal mol^{-1})	ΔS (cal mol^{-1} K^{-1})	ΔG° (kcal mol^{-1})	$\Delta\Delta G^\circ$ (kcal mol^{-1})	T_m (°C)	ΔT_m (°C)
11-S:AS-L9	*acgaccagagttacag*	*ctgtaactCtggtcgt*	DNA:LNA	118.8 ± 1.3 (132.5)	318.4 ± 3.6 (360.1)	14.66 ± 0.14 (14.83)	1.12 ± 0.18	70.9 ± 0.2 (69.0)	3.5 ± 0.2
11-S:AS-L11	*acgaccagagttacag*	*ctgtaactctGgtcgt*	DNA:LNA	119.7 ± 0.9 (131.9)	320.8 ± 2.7 (359.4)	14.78 ± 0.03 (14.50)	1.24 ± 0.11	71.1 ± 0.1 (68.1)	3.8 ± 0.1
11-S:AS-L12	*acgaccagagttacag*	*ctgtaactctgGtcgt*	DNA:LNA	114.4 ± 1.5 (131.9)	306.0 ± 4.4 (359.4)	14.27 ± 0.07 (14.50)	0.73 ± 0.13	70.3 ± 0.0 (68.1)	3.0 ± 0.0
11-S-L3:AS	*acGaccagagttacag*	*ctgtaactctggtcgt*	LNA:DNA	116.2 ± 2.2 (131.9)	313.6 ± 6.4 (359.4)	13.69 ± 0.10 (14.50)	0.15 ± 0.15	68.0 ± 0.0 (68.1)	0.7 ± 0.1
11-S-L4:AS	*acgAccagagttacag*	*ctgtaactctggtcgt*	LNA:DNA	115.8 ± 0.0 (131.4)	311.1 ± 0.0 (358.8)	14.12 ± 0.01 (14.23)	0.58 ± 0.11	69.5 ± 0.0 (67.4)	2.2 ± 0.1
11-S-L5:AS	*acgaCcagagttacag*	*ctgtaactctggtcgt*	LNA:DNA	113.0 ± 0.6 (132.5)	301.1 ± 1.7 (360.1)	14.50 ± 0.02 (14.83)	0.96 ± 0.11	71.4 ± 0.1 (69.0)	4.0 ± 0.1
11-S-L6:AS	*acgacCagagttacag*	*ctgtaactctggtcgt*	LNA:DNA	113.3 ± 2.3 (132.5)	302.7 ± 6.6 (360.1)	14.25 ± 0.12 (14.83)	0.71 ± 0.16	70.4 ± 0.0 (69.0)	3.1 ± 0.1
11-S-L9:AS	*acgaccagAgttacag*	*ctgtaactctggtcgt*	LNA:DNA	112.0 ± 1.5 (131.4)	298.0 ± 4.3 (358.8)	14.48 ± 0.07 (14.23)	0.94 ± 0.13	71.5 ± 0.0 (67.4)	4.2 ± 0.1
11-S-L10:AS	*acgaccagaGttacag*	*ctgtaactctggtcgt*	LNA:DNA	110.2 ± 1.8 (131.9)	294.3 ± 5.1 (359.4)	13.96 ± 0.10 (14.50)	0.42 ± 0.15	69.9 ± 0.0 (68.1)	2.6 ± 0.1
11-S-L11:AS	*acgaccagagTtacag*	*ctgtaactctggtcgt*	LNA:DNA	111.6 ± 1.7 (132.0)	298.2 ± 4.9 (359.5)	14.00 ± 0.09 (14.55)	0.46 ± 0.14	69.8 ± 0.1 (68.3)	2.5 ± 0.1
11-S-L12:AS	*acgaccagagtTacag*	*ctgtaactctggtcgt*	LNA:DNA	113.1 ± 1.1 (132.0)	302.3 ± 3.1 (359.5)	14.23 ± 0.05 (14.55)	0.69 ± 0.12	70.4 ± 0.0 (68.3)	3.0 ± 0.1

Values reported in parentheses are the corresponding melting thermodynamics predicted by the standard SBT model. Duplex names, for example 1-S-L3:AS, indicate the number (name) of the isosequential pure-DNA duplex (e.g., 1), the LNA content of the sense (S) strand (L3, which indicates an LNA at the 5′+3 nucleotide position), and the LNA content of the antisense (AS) strand (the AS strand has no LNA substitution in the 1-S-L3:AS duplex). The reported UVM data ($\Delta H(T_m)$, $\Delta S(T_m)$, ΔG°, and T_m) are for the helix-to-coil transition and were determined as reported in Materials and Methods. The reported errors refer to the standard deviation of the triplicate runs. All duplex samples were resuspended in buffer containing 1 M NaCl, 10 mM Na_2HPO_4, and 1 mM Na_2EDTA (pH = 7.0). Pure DNA or LNA bearing duplexes isosequential to sequences 1–7 or 8–11 were resuspended to a C_T of 7.5 or 5 μM, respectively.

[a]Duplex sequences were previously studied by Hughesman et al.[19]

[b]Duplex sequences were previously studied by Hughesman et al.[41]

[c]Duplex sequences were previously studied by McTigue et al.[21]

Table 2. Melting Thermodynamic Data Collected by UV Spectroscopy for the "Learning Set" of Complementary Duplexes Bearing an LNA Substitution Within Both Strands

Duplex Name	*Sense Strand* (5′−3′)	*Antisense Strand* (5′−3′)	ΔH (kcal mol^{-1})	ΔS (cal mol^{-1} K^{-1})	ΔG^o (kcal mol^{-1})	$\Delta\Delta G^o$ (kcal mol^{-1})	T_m (°C)	ΔT_m (°C)	$\Delta\Delta T_m$ (°C)
1-S-L5:AS-L7	*ttcaTagccgt*	*acggctAtgaa*	75.4 ± 1.3	199.1 ± 4.0	10.41 ± 0.05 (10.50)	1.68 ± 0.07	61.5 ± 0.1 (61.1)	7.7 ± 0.3 (7.4)	1.8 (0.9)
1-S-L6:AS-L6	*ttcatAgccgt*	*acggcTatgaa*	77.4 ± 0.6	204.1 ± 1.9	10.78 ± 0.01 (10.50)	2.05 ± 0.05	63.0 ± 0.2 (61.1)	9.2 ± 0.3 (7.4)	1.6 (0.9)
1-S-L7:AS-L5	*ttcataGccgt*	*acggCtatgaa*	73.6 ± 1.2	192.7 ± 3.5	10.64 ± 0.07 (11.03)	1.92 ± 0.09	62.9 ± 0.2 (63.2)	9.1 ± 0.3 (9.5)	−0.3 (0.9)
1-S-L8:AS-L4	*ttcatagCcgt*	*acgGctatgaa*	79.0 ± 1.9	208.1 ± 5.7	11.03 ± 0.09 (11.03)	2.30 ± 0.10	63.9 ± 0.1 (63.2)	10.2 ± 0.3 (9.5)	1.2 (0.9)
1-S-L4:AS-L8	*ttcAtagccgt*	*acggctaTgaa*	85.7 ± 0.4	230.5 ± 1.1	10.44 ± 0.02 (10.50)	1.71 ± 0.05	60.5 ± 0.0 (61.1)	6.8 ± 0.2 (7.4)	1.7 (0.9)
1-S-L6:AS-L5	*ttcatAgccgt*	*acggCtatgaa*	72.9 ± 2.1	189.7 ± 6.2	10.88 ± 0.11 (11.09)	2.16 ± 0.12	64.2 ± 0.2 (63.4)	10.5 ± 0.3 (9.7)	0.6 (2.2)
1-S-L7:AS-L4	*ttcataGccgt*	*acgGctatgaa*	71.9 ± 1.8	188.2 ± 5.3	10.47 ± 0.09 (11.03)	1.75 ± 0.10	62.3 ± 0.2 (63.1)	8.5 ± 0.3 (9.5)	2.1 (2.2)
1-S-L5:AS-L6	*ttcaTagccgt*	*acggcTatgaa*	81.8 ± 1.9	215.3 ± 5.5	11.48 ± 0.10 (11.14)	2.75 ± 0.12	65.6 ± 0.2 (63.7)	11.8 ± 0.3 (10.0)	2.8 (2.2)
1-S-L4:AS-L7	*ttcAtagccgt*	*acggctAtgaa*	79.1 ± 0.3	211.6 ± 1.0	10.04 ± 0.02 (10.51)	1.31 ± 0.05	59.4 ± 0.1 (61.0)	5.6 ± 0.2 (7.3)	1.7 (2.2)
1-S-L3:AS-L8	*ttCatagccgt*	*acggctaTgaa*	81.7 ± 1.0	215.9 ± 3.0	11.15 ± 0.05 (11.41)	2.43 ± 0.07	64.1 ± 0.1 (64.8)	10.4 ± 0.2 (11.1)	2.9 (2.2)
1-S-L5:AS-L5	*ttcaTagccgt*	*acggCtatgaa*	86.6 ± 1.7	228.7 ± 4.9	11.90 ± 0.08 (11.51)	3.18 ± 0.09	66.7 ± 0.1 (65.2)	12.9 ± 0.2 (11.5)	1.7 (2.6)
1-S-L4:AS-L6	*ttcAtagccgt*	*acggcTatgaa*	79.5 ± 0.9	210.7 ± 2.6	10.73 ± 0.07 (10.92)	2.00 ± 0.09	62.5 ± 0.2 (62.7)	8.7 ± 0.3 (9.0)	1.7 (2.6)
1-S-L6:AS-L4	*ttcatAgccgt*	*acgGctatgaa*	78.5 ± 0.6	206.9 ± 1.8	10.91 ± 0.02 (10.87)	2.19 ± 0.06	63.5 ± 0.1 (62.5)	9.7 ± 0.2 (8.8)	2.9 (2.6)
1-S-L3:AS-L7	*ttCatagccgt*	*acggctAtgaa*	87.0 ± 0.3	232.2 ± 1.0	11.17 ± 0.03 (11.19)	2.45 ± 0.06	63.5 ± 0.1 (63.8)	9.7 ± 0.2 (10.1)	3.4 (2.6)
1-S-L3:AS-L6	*ttCatagccgt*	*acggcTatgaa*	80.7 ± 1.0	212.6 ± 2.8	11.25 ± 0.06 (11.21)	2.53 ± 0.08	64.7 ± 0.1 (64.0)	11.0 ± 0.2 (10.3)	1.6 (1.4)
1-S-L5:AS-L4	*ttcaTagccgt*	*acgGctatgaa*	87.6 ± 3.9	233.4 ± 11.4	11.40 ± 0.22 (10.89)	2.68 ± 0.22	64.3 ± 0.4 (62.7)	10.6 ± 0.4 (9.0)	2.4 (1.4)
1-S-L4:AS-L5	*ttcAtagccgt*	*acggCtatgaa*	77.2 ± 2.8	204.0 ± 8.3	10.60 ± 0.14 (10.90)	1.87 ± 0.15	62.1 ± 0.3 (62.7)	8.4 ± 0.4 (9.0)	−0.8 (1.4)
1-S-L4:AS-L4	*ttcAtagccgt*	*acgGctatgaa*	72.6 ± 3.9	192.3 ± 11.3	9.87 ± 0.18 (10.32)	1.14 ± 0.19	59.2 ± 0.2 (60.3)	5.4 ± 0.3 (6.6)	−0.8 (0.4)
1-S-L3:AS-L5	*ttCatagccgt*	*acggCtatgaa*	88.2 ± 0.3	234.2 ± 1.0	11.74 ± 0.01 (11.23)	3.01 ± 0.05	65.7 ± 0.0 (64.1)	11.9 ± 0.2 (10.4)	0.4 (0.4)
1-S-L4:AS-L9	*ttcAtagccgt*	*acggctatGaa*	77.5 ± 2.2	208.1 ± 6.5	9.59 ± 0.07 (10.16)	0.86 ± 0.09	57.5 ± 0.2 (59.7)	3.7 ± 0.3 (6.0)	0.7 (−0.2)
1-S-L5:AS-L8	*ttcaTagccgt*	*acggctaTgaa*	78.9 ± 1.8	210.8 ± 5.2	10.10 ± 0.07 (10.53)	1.37 ± 0.09	59.7 ± 0.1 (61.3)	5.9 ± 0.3 (7.6)	−1.2 (−0.2)
1-S-L6:AS-L7	*ttcatAgccgt*	*acggctAtgaa*	75.9 ± 1.1	201.1 ± 2.8	10.27 ± 0.05 (9.90)	1.54 ± 0.07	59.4 ± 0.1 (58.6)	5.6 ± 0.3 (4.9)	1.1 (−0.2)
1-S-L7:AS-L6	*ttcataGccgt*	*acggcTatgaa*	72.7 ± 2.3	191.5 ± 6.8	10.22 ± 0.09 (10.48)	1.49 ± 0.10	60.9 ± 0.2 (61.0)	7.1 ± 0.3 (7.3)	−0.1 (−0.2)
1-S-L8:AS-L5	*ttcatagCcgt*	*acggCtatgaa*	76.1 ± 0.3	199.6 ± 1.0	10.91 ± 0.02 (11.08)	2.18 ± 0.05	63.8 ± 0.0 (63.4)	10 ± 0.2 (9.7)	−1.9 (−0.2)
1-S-L6:AS-L8	*ttcatAgccgt*	*acggctaTgaa*	77.7 ± 2.3	207.8 ± 6.9	9.87 ± 0.08 (10.05)	1.15 ± 0.09	58.8 ± 0.2 (59.2)	5 ± 0.3 (5.5)	−0.7 (−0.9)

TABLE 2. *Continued*

Duplex Name	*Sense Strand* (5′−3′)	*Antisense Strand* (5′−3′)	ΔH (kcal mol^{-1})	ΔS (cal mol^{-1} K^{-1})	ΔG^o (kcal mol^{-1})	$\Delta\Delta G^o$ (kcal mol^{-1})	T_m (°C)	ΔT_m (°C)	$\Delta\Delta T_m$ (°C)
1-S-L7:AS-L7	*ttcataGccgt*	*acggctAtgaa*	85.4 ± 1.5	231.3 ± 4.4	9.98 ± 0.06 (10.00)	1.25 ± 0.08	58.6 ± 0.1 (59.0)	4.9 ± 0.3 (5.3)	0.8 (−0.9)
1-S-L8:AS-L6	*ttcatagCcgt*	*acggcTatgaa*	85.5 ± 2.6	227.8 ± 7.7	11.16 ± 0.11 (10.64)	2.43 ± 0.12	63.6 ± 0.1 (61.7)	9.8 ± 0.2 (8.0)	0.0 (−0.9)
1-S-L7:AS-L8	*ttcataGccgt*	*acggctaTgaa*	86.7 ± 3.8	234.7 ± 11.3	10.15 ± 0.09 (10.41)	1.42 ± 0.10	59.2 ± 0.1 (60.8)	5.5 ± 0.2 (7.1)	0.2 (−0.5)
1-S-L8:AS-L7	*ttcatagCcgt*	*acggctAtgaa*	85.3 ± 0.9	229.3 ± 2.7	10.52 ± 0.04 (10.42)	1.80 ± 0.07	60.9 ± 0.1 (60.8)	7.2 ± 0.2 (7.1)	0.5 (−0.5)
2-S-L7:AS-L3	*tgcggaTaagt*	*acTtatccgca*	83.4 ± 2.5	222.3 ± 7.4	10.88 ± 0.10 (11.23)	2.12 ± 0.11	62.6 ± 0.2 (64.1)	8.8 ± 0.2 (10.4)	3.5 (2.6)
2-S-L9:AS-L5	*tgcggataAgt*	*acttAtccgca*	79.7 ± 3.7	213.9 ± 10.7	9.94 ± 0.15 (9.73)	1.18 ± 0.15	58.9 ± 0.4 (57.9)	5.1 ± 0.4 (4.2)	−0.5 (−0.9)
3-S-L4:AS-L8	*ctaAcggatgc*	*gcatccgTtag*	82.0 ± 3.7	221.1 ± 11.0	9.87 ± 0.13 (10.40)	1.12 ± 0.14	58.4 ± 0.3 (60.2)	4.6 ± 0.4 (7.0)	−1.4 (0.9)
3-S-L5:AS-L7	*ctaaCggatgc*	*gcatccGttag*	78.8 ± 1.6	209.1 ± 4.6	10.50 ± 0.06 (10.93)	1.75 ± 0.08	61.5 ± 0.1 (62.3)	7.7 ± 0.2 (9.0)	−0.1 (0.9)
3-S-L6:AS-L6	*ctaacGgatgc*	*gcatcCgttag*	77.1 ± 0.4	203.0 ± 1.1	10.84 ± 0.03 (10.93)	2.09 ± 0.05	63.3 ± 0.1 (62.3)	9.5 ± 0.2 (9.0)	0.5 (0.9)
3-S-L7:AS-L5	*ctaacgGatgc*	*gcatCcgttag*	75.9 ± 1.7	199.1 ± 5.1	10.89 ± 0.12 (10.93)	2.14 ± 0.13	63.8 ± 0.6 (62.3)	9.9 ± 0.6 (9.0)	−0.3 (0.9)
3-S-L8:AS-L4	*ctaacggAtgc*	*gcaTccgttag*	78.9 ± 1.1	211.1 ± 3.4	10.01 ± 0.03 (10.40)	1.26 ± 0.05	59.3 ± 0.1 (60.2)	5.4 ± 0.2 (7.0)	−1.2 (0.9)
3-S-L4:AS-L7	*ctaAcggatgc*	*gcatccGttag*	83.8 ± 3.4	224.6 ± 9.5	10.50 ± 0.27 (10.67)	1.75 ± 0.27	60.9 ± 0.8 (61.2)	7.1 ± 0.8 (7.9)	0.7 (2.1)
3-S-L5:AS-L6	*ctaaCggatgc*	*gcatcCgttag*	76.0 ± 0.7	197.4 ± 2.0	11.48 ± 0.03 (11.58)	2.73 ± 0.05	66.7 ± 0.0 (64.8)	12.8 ± 0.2 (11.5)	3.6 (2.1)
3-S-L6:AS-L5	*ctaacGgatgc*	*gcatCcgttag*	75.1 ± 1.9	195.8 ± 5.3	11.17 ± 0.11 (11.26)	2.42 ± 0.11	65.3 ± 0.2 (63.5)	11.4 ± 0.3 (10.2)	2.6 (2.1)
3-S-L7:AS-L4	*ctaacgGatgc*	*gcaTccgttag*	74.1 ± 2.7	193.5 ± 7.7	10.90 ± 0.14 (10.98)	2.15 ± 0.15	64.1 ± 0.3 (62.5)	10.3 ± 0.3 (9.2)	1.6 (2.1)
3-S-L4:AS-L6	*ctaAcggatgc*	*gcatcCgttag*	80.2 ± 0.8	211.8 ± 2.4	11.03 ± 0.05 (11.09)	2.28 ± 0.06	63.8 ± 0.1 (62.9)	9.9 ± 0.2 (9.6)	2.0 (2.5)
3-S-L5:AS-L5	*ctaaCggatgc*	*gcatCcgttag*	75.3 ± 2.6	195.9 ± 7.6	11.28 ± 0.14 (11.68)	2.54 ± 0.15	65.8 ± 0.2 (65.2)	12 ± 0.3 (11.9)	2.9 (2.4)
3-S-L6:AS-L4	*ctaacGgatgc*	*gcaTccgttag*	78.4 ± 1.3	206.5 ± 3.6	10.96 ± 0.07 (11.08)	2.21 ± 0.08	63.7 ± 0.2 (62.9)	9.9 ± 0.2 (9.6)	2.6 (2.5)
3-S-L4:AS-L5	*ctaAcggatgc*	*gcatCcgttag*	82.1 ± 5.1	216.2 ± 17.6	11.53 ± 0.54 (10.79)	2.78 ± 0.54	62.4 ± 0.7 (61.8)	8.6 ± 0.7 (8.5)	0.9 (1.3)
3-S-L5:AS-L4	*ctaaCggatgc*	*gcaTccgttag*	80.0 ± 0.4	211.0 ± 1.1	11.11 ± 0.02 (11.11)	2.37 ± 0.05	64.2 ± 0 (63.0)	10.3 ± 0.2 (9.8)	2.8 (1.3)
3-S-L5:AS-L8	*ctaaCggatgc*	*gcatccgTtag*	76.1 ± 0.3	202.1 ± 8.8	10.17 ± 0.12 (10.70)	1.42 ± 0.13	60.3 ± 0.3 (61.5)	6.4 ± 0.3 (8.2)	−0.9 (−0.2)
3-S-L6:AS-L7	*ctaacGgatgc*	*gcatccGttag*	77.7 ± 1.7	206.3 ± 5.1	10.38 ± 0.08 (10.32)	1.63 ± 0.09	61.1 ± 0.2 (59.9)	7.2 ± 0.3 (6.7)	−0.3 (−0.2)
3-S-L7:AS-L6	*ctaacgGatgc*	*gcatcCgttag*	74.1 ± 2.7	193.5 ± 7.7	10.90 ± 0.14 (10.65)	2.15 ± 0.15	64.1 ± 0.3 (61.2)	10.3 ± 0.3 (8.0)	−0.1 (−0.2)

TABLE 2. *Continued*

Duplex Name	*Sense Strand* (5′−3′)	*Antisense Strand* (5′−3′)	ΔH (kcal mol^{-1})	ΔS (cal mol^{-1} K^{-1})	ΔG^o (kcal mol^{-1})	$\Delta\Delta G^o$ (kcal mol^{-1})	T_m (°C)	ΔT_m (°C)	$\Delta\Delta T_m$ (°C)
3-S-L8:AS-L5	*ctaacggAtgc*	*gcatCcgttag*	76.5 ± 1.5	203.0 ± 4.5	10.31 ± 0.06 (10.39)	1.56 ± 0.07	60.9 ± 0.1 (60.2)	7.0 ± 0.2 (6.9)	−1.1 (−0.2)
3-S-L4:AS-L9	*ctaAcggatgc*	*gcatccgtTag*	82.5 ± 1.6	222.0 ± 4.6	10.06 ± 0.05 (10.11)	1.31 ± 0.07	59.2 ± 0.1 (59.2)	5.4 ± 0.2 (5.9)	−0.4 (−0.2)
3-S-L6:AS-L8	*ctaacGgatgc*	*gcatccgTtag*	82.2 ± 0.8	220.8 ± 2.5	10.20 ± 0.02 (10.21)	1.45 ± 0.05	59.8 ± 0.0 (59.5)	6.0 ± 0.2 (6.3)	−1.0 (−0.9)
3-S-L8:AS-L6	*ctaacggAtgc*	*gcatcCgttag*	78.1 ± 1.2	207.4 ± 3.9	10.44 ± 0.04 (10.22)	1.69 ± 0.06	60.8 ± 0.1 (59.5)	7.0 ± 0.2 (6.3)	−1.3 (−0.9)
3-S-L6:AS-L7	*ctaacgGatgc*	*gcatccGttag*	79.7 ± 0.7	212.8 ± 2.2	10.28 ± 0.02 (10.16)	1.53 ± 0.05	60.8 ± 0.6 (59.3)	7.0 ± 0.7 (6.0)	−1.9 (−0.9)
3-S-L8:AS-L7	*ctaacggAtgc*	*gcatccGttag*	78.1 ± 1.9	209.5 ± 5.8	9.74 ± 0.07 (10.00)	0.99 ± 0.08	58.1 ± 0.2 (58.7)	4.3 ± 0.2 (5.4)	−2.6 (−0.5)
3-S-L6:AS-L8	*ctaacgGatgc*	*gcatccgTtag*	77.7 ± 2.2	206.2 ± 6.3	10.43 ± 0.10 (10.31)	1.68 ± 0.11	61.3 ± 0.2 (60.0)	7.5 ± 0.3 (6.7)	−1.0 (−0.5)
4-S-L6:AS-L6	*ctacgCattcc*	*ggaatGcgtag*	79.3 ± 1.8	209.3 ± 5.3	10.97 ± 0.06 (10.93)	2.31 ± 0.09	63.6 ± 0.0 (62.3)	10.2 ± 0.3 (9.0)	1.6 (0.9)
4-S-L8:AS-L3	*ctacgcatTcc*	*ggAatgcgtag*	87.6 ± 3.8	234.5 ± 11.3	11.01 ± 0.13 (10.40)	2.36 ± 0.15	62.7 ± 0.1 (60.2)	9.3 ± 0.3 (7.0)	2.0 (0.9)
4-S-L4:AS-L8	*ctaCgcattcc*	*ggaatgcGtag*	84.1 ± 0.4	223.8 ± 1.2	10.99 ± 0.01 (10.93)	2.34 ± 0.07	63.1 ± 0.0 (62.3)	9.6 ± 0.3 (9.0)	2.3 (0.9)
4-S-L7:AS-L5	*ctacgcAttcc*	*ggaaTgcgtag*	79.8 ± 1.4	211.7 ± 4.0	10.67 ± 0.07 (10.40)	2.01 ± 0.09	62.2 ± 0.1 (60.2)	8.7 ± 0.3 (7.0)	2.9 (2.1)
4-S-L8:AS-L3	*ctacgcaTtcc*	*ggAatgcgtag*	82.4 ± 1.5	219.4 ± 4.4	10.75 ± 0.07 (10.72)	2.10 ± 0.10	62.2 ± 0.1 (61.5)	8.8 ± 0.3 (8.2)	2.6 (2.5)
4-S-L7:AS-L3	*ctacgcAttcc*	*ggAatgcgtag*	77.0 ± 1.8	204.0 ± 5.4	10.41 ± 0.07 (10.50)	1.76 ± 0.09	61.3 ± 0.1 (60.6)	7.9 ± 0.3 (7.3)	3.3 (2.4)
4-S-L4:AS-L6	*ctaCgcattcc*	*ggaatGcgtag*	81.4 ± 0.4	215.1 ± 1.2	11.13 ± 0.01 (11.35)	2.48 ± 0.07	64.1 ± 0.0 (63.9)	10.6 ± 0.3 (10.6)	3.9 (1.3)
4-S-L4:AS-L5	*ctaCgcattcc*	*ggaaTgcgtag*	85.8 ± 0.4	227.7 ± 1.0	11.46 ± 0.04 (11.11)	2.80 ± 0.07	64.8 ± 0.1 (63.0)	11.4 ± 0.3 (9.8)	2.7 (−0.9)
4-S-L9:AS-L5	*ctacgcatTcc*	*ggaaTgcgtag*	76.8 ± 4.3	204.0 ± 12.5	10.24 ± 0.18 (10.26)	1.59 ± 0.19	60.5 ± 0.4 (59.8)	7.1 ± 0.5 (6.5)	−1.4 (−0.9)
4-S-L6:AS-L8	*ctacgCattcc*	*ggaatgcGtag*	81.0 ± 1.7	214.8 ± 4.1	10.91 ± 0.06 (10.49)	2.25 ± 0.09	61.1 ± 0.6 (60.6)	7.7 ± 0.7 (7.3)	−1.5 (−0.9)
5-S-L8:AS-L6	*ctattggCgac*	*gtcgcCaatag*	82.1 ± 3.0	218.3 ± 6.3	10.88 ± 0.26 (10.81)	1.64 ± 0.26	62.8 ± 0.9 (61.9)	7.0 ± 0.9 (8.6)	−1.0 (−0.9)
6-S-L6:AS-L6	*ctgaaGtccgc*	*gcggaCttcag*	82.9 ± 0.6	216.6 ± 1.8	12.12 ± 0.04 (12.04)	2.33 ± 0.11	68.4 ± 0.0 (66.4)	10.3 ± 0.2 (8.9)	−0.7 (0.8)
6-S-L6:AS-L4	*ctgaaGtccgc*	*gcgGacttcag*	84.2 ± 0.9	220.7 ± 2.5	12.07 ± 0.05 (12.14)	2.27 ± 0.11	67.9 ± 0.0 (66.7)	9.8 ± 0.2 (9.2)	0.7 (2.4)
6-S-L6:AS-L3	*ctgaaGtccgc*	*gcGgacttcag*	85.9 ± 0.8	226.9 ± 2.2	11.76 ± 0.03 (11.84)	1.96 ± 0.11	66.2 ± 0.1 (65.6)	8.1 ± 0.2 (8.1)	1.2 (1.3)
6-S-L4:AS-L5	*ctgAagtccgc*	*gcggActtcag*	87.3 ± 0.3	229.9 ± 1.0	12.18 ± 0.02 (11.32)	2.39 ± 0.11	67.8 ± 0.0 (63.6)	9.7 ± 0.2 (6.1)	0.4 (1.3)
6-S-L5:AS-L4	*ctgaAgtccgc*	*gcgGacttcag*	85.3 ± 2.2	223.1 ± 6.4	12.39 ± 0.14 (11.58)	2.59 ± 0.17	69.1 ± 0.1 (64.6)	11.0 ± 0.2 (7.1)	0.7 (1.3)

TABLE 2. *Continued*

Duplex Name	*Sense Strand* (5′−3′)	*Antisense Strand* (5′−3′)	ΔH (kcal mol^{-1})	ΔS (cal mol^{-1} K^{-1})	ΔG^o (kcal mol^{-1})	$\Delta\Delta G^o$ (kcal mol^{-1})	T_m (°C)	ΔT_m (°C)	$\Delta\Delta T_m$ (°C)
6-S-L3:AS-L6	*ctGaagtccgc*	*gcggaCttcag*	92.0 ± 1.3	244.6 ± 3.7	12.12 ± 0.06 (12.17)	2.32 ± 0.12	66.7 ± 0.1 (66.9)	8.6 ± 0.2 (9.4)	0.9 (1.3)
6-S-L3:AS-L5	*ctGaagtccgc*	*gcggActtcag*	87.2 ± 1.8	232.1 ± 5.3	11.43 ± 0.10 (11.33)	1.64 ± 0.14	64.5 ± 0.2 (63.7)	6.4 ± 0.3 (6.2)	0.7 (0.4)
7-S-L3:AS-L6	*gtAtcaagtct*	*agactTgatac*	85.0 ± 0.9	232.9 ± 2.8	9.01 ± 0.03 (8.50)	1.86 ± 0.04	54.8 ± 0.1 (52.8)	7.5 ± 0.3 (8.1)	0.9 (1.5)
7-S-L4:AS-L5	*gtaTcaagtct*	*agacTtgatac*	82.6 ± 1.0	225.4 ± 3.0	9.06 ± 0.02 (8.81)	1.92 ± 0.03	55.1 ± 0.1 (54.2)	7.8 ± 0.2 (9.5)	1.4 (1.5)
7-S-L5:AS-L4	*gtatCaagtct*	*agaCttgatac*	80.8 ± 1.0	216.7 ± 3.1	10.07 ± 0.04 (9.36)	2.92 ± 0.04	59.4 ± 0.1 (56.4)	12.1 ± 0.2 (11.7)	1.3 (1.5)

These data were globally fit to the extended SBT model using the LM method to regress the required set of $\Delta\Delta G^{o}_{\text{hyper-}(j)}$ parameters. Values reported in parenthesis are the corresponding melting thermodynamics predicted by the extended SBT model. The reported UVM data ($\Delta H(T_m)$, $\Delta S(T_m)$, ΔG^o, and T_m) are for the helix-to-coil transition and were determined as reported in Materials and Methods. The reported errors refer to the standard deviation of triplicate runs. All duplex samples were resuspended in buffer containing 1 M NaCl, 10 mM Na_2HPO_4, and 1 mM Na_2EDTA (pH = 7.0) to a $C_T = 7.5$ μM.

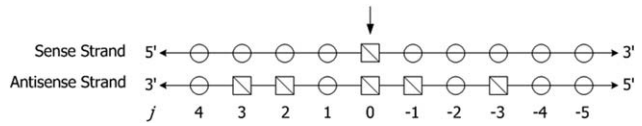

Figure 2. General structure of the library of complementary duplexes created to study changes in thermal stability arising from an LNA substitution within each strand.

Standard DNA nucleotides and LNA-substituted nucleotides are indicated by circles and squares, respectively. The position of each LNA on the antisense strand is indexed relative to a selected LNA (arrow) on the sense strand by the value of j, where $-4 \le j \le 3$ in this study. In this example, the duplex has an LNA:LNA base pair ($j = 0$), and oppositely oriented DNA:LNA base pairs at positions $j = 3$, 2, −1, and −3 of the antisense strand.

an LNA:LNA base pair and oppositely oriented LNA:DNA base pairs

Sense strand 5′ *c a t a C g a t g* 3′

Antisense strand 3′ *g t A t G C T a c* 5′

where lower-case letters indicate standard DNA nucleotides, and capital letters the corresponding LNAs. The LNA on the sense strand is selected, and the relative position of each LNA on the antisense strand is noted. For the *C* at the 5′+5 position of the sense strand, they include the *G* with which it is paired ($j = 0$; $n_j = n_0 = 1$ as there is only one *C*:*G* LNA-LNA base pair in the duplex), the adjacent *C* ($j = -1$; $n_{-1} = 1$) on the 5′-side of the *G* on the antisense strand, and the *A* and *T* that are in the $j = +2$ and $j = -2$ positions, respectively, of the antisense strand. When required, the same analysis would be performed for any additional LNA on the sense strand. Application of Eq. 13 for the example duplex shown (for which all $n_j = 1$ in this case) above then gives

$$\Delta\Delta G^{\text{o}}_{\text{hyper}} = \Delta\Delta G^{\text{o}}_{\text{hyper}-(2)} + \Delta\Delta G^{\text{o}}_{\text{hyper}-(0)} + \Delta\Delta G^{\text{o}}_{\text{hyper}-(-1)} + \Delta\Delta G^{\text{o}}_{\text{hyper}-(-2)} \quad (14)$$

The set of $\Delta\Delta G^{o}_{\text{hyper}-(j)}$ parameters required to compute $\Delta\Delta G^{\text{o}}_{\text{hyper}}$ were found by global iterative regression of the model to a large set (see below) of $\Delta\Delta T_{m\,(\text{exp}t)}$ data using the LM method until a minimum in χ^2 was achieved. Each experimental T_m used to determine both $\Delta\Delta T_{m\,(\text{exp}t)}$ and model parameters represents the mean of triplicate independent runs, and is reported along with its standard deviation, which was used to compute errors in each regressed parameter.

Results

Standard SBT model and its performance when applied to duplexes containing any number and pattern of LNA substitutions within one strand

The standard SBT model uses an experimental ΔC_p^{bp} value (42 cal mol^{-1} K^{-1} bp^{-1}) and a set of four incremental entropy parameters ($\Delta\Delta S_i^o$) to compute sequence-specific melting thermodynamics and T_m for any short DNA duplex bearing any number and pattern of LNA substitutions on one of the two strands. Thermodynamic changes (ΔH_{LNA} and ΔS_{LNA}) for the helix-to-coil transition at T_m are predicted using Eqs. 11 and 12 with $\Delta\Delta H^o_{\text{LNA}}$ set equal to zero and $\Delta\Delta S^o_{\text{LNA}}$ given by

$$\Delta\Delta S^{\text{o}}_{\text{LNA}} = \sum n_i \Delta\Delta S^{\text{o}}_i \quad (15)$$

Table 3. Melting Thermodynamic Data Collected by UV Spectroscopy for a Set of Duplexes Having the Pure-DNA Sequence 5′-*ggaacaagatgc*-3′ and Varying LNA Content

	DNA Duplex	T_m (°C)	ΔT_m (°C)	$\Delta\Delta T_m$ (°C)		DNA Duplex	T_m (°C)	ΔT_m (°C)	$\Delta\Delta T_m$ (°C)
10	5′ g g a a c a a g a t g c 3′ 3′ c c t t g t t c t a c g 5′	54.6							
Parent DNA Duplexes with Single LNA Substitutions on a Single Strand									
10-S-L7:AS	5′ g g a a c a A g a t g c 3′ 3′ c c t t g t t c t a c g 5′	58.1	3.5		10-S-L6:AS	5′ g g a a c A a g a t g c 3′ 3′ c c t t g t t c t a c g 5′	56.0	1.4	
10-S-L9:AS	5′ g g a a c a a g A t g c 3′ 3′ c c t t g t t c t a c g 5′	57.2	2.6		10-S:AS-L6	5′ g g a a c a a g a t g c 3′ 3′ c c t t g t T c t a c g 5′	57.2	2.6	
10-S:AS-L5	5′ g g a a c a a g a t g c 3′ 3′ c c t t g t t C t a c g 5′	59.6	5.0		10-S:AS-L7	5′ g g a a c a a g a t g c 3′ 3′ c c t t g T t c t a c g 5′	58.9	4.3	
DNA Duplexes with Multiple LNA Substitutions on a Single Strand									
10-S-L79:AS	5′ g g a a c a A g A t g c 3′ 3′ c c t t g t t c t a c g 5′	61.4	6.8	(6.1)	10-S:AS-L67	5′ g g a a c a a g a t g c 3′ 3′ c c t t g T T c t a c g 5′	61.6	7.0	(6.9)
DNA Duplexes with Single LNA Substitutions on Opposing Strands									
10-S-L7:AS-L5	5′ g g a a c a A g a t g c 3′ 3′ c c t t g t t C t a c g 5′	64.5	10.0	(8.5)	1.5	10-S-L6:AS-L7	5′ g g a a c A a g a t g c 3′ 3′ c c t t g T t c t a c g 5′	62.3	7.7	(5.7) 1.9
10-S-L9:AS-L5	5′ g g a a c a a g A t g c 3′ 3′ c c t t g t t C t a c g 5′	61.9	7.3	(7.6)	-0.3	10-S-L6:AS-L6	5′ g g a a c A a g a t g c 3′ 3′ c c t t g t T c t a c g 5′	61.0	6.4	(4.0) 2.3
DNA Duplexes with Multiple LNA Substituions on Opposing Strands									
10-S-L79:AS-L5	5′ g g a a c a A g A t g c 3′ 3′ c c t t g t t C t a c g 5′	67.6	13.0	(11.8)	1.2 (1.2)	10-S-L6:AS-L67	5′ g g a a c A a g a t g c 3′ 3′ c c t t g T T c t a c g 5′	66.7	12.1	(8.4) 3.7 (4.2)

where n_i is the number (frequency) of internal LNA substitutions of type i (i.e., not including those at either terminus), and the values of $\Delta\Delta S_i^o$ are specific to the reference temperature. The value of T_m for any duplex in which one strand contains one or more LNA substitutions is then given by Eq. 5 with $\Delta H = \Delta H_{\mathrm{LNA}}$ and $\Delta S = \Delta S_{\mathrm{LNA}}$. Because of the temperature dependencies of ΔH_{LNA} and ΔS_{LNA}, the solution of Eq. 5 requires iteration, but convergence is rapid if an initial estimate for T_m is found by setting $\Delta C_p = 0$ in Eqs. 11 and 12.

To date, the standard SBT model has been tested on a relatively small set of complementary duplexes bearing LNA substitutions on one strand. We, therefore, sought to further validate model performance when applied to that class of duplexes by collecting melting thermodynamics and T_m data for a large set of duplexes containing different patterns of LNA substitutions on one strand, and then comparing model predictions to the resulting dataset. Those melting thermodynamics data are reported in Table 1, and we note that none of the sequences and associated data was used in the regression of the previously reported standard SBT model parameters.

The corresponding standard SBT model predictions for each of the pure-DNA and LNA-substituted duplexes are also reported. The results confirm that the model accurately predicts both melting thermodynamics and T_m, irrespective of the pattern and frequency of LNA substitutions within the one strand. For the entire set of LNA-substituted duplexes, the standard SBT model predicts ΔH, ΔS, and T_m values with a mean error and standard deviation of 3.0 ± 7.1 kcal mol^{-1}, 9.6 ± 21.2 cal mol^{-1} K^{-1}, and -0.9 ± 1.4°C, respectively. Each of these errors is essentially equivalent to the corresponding error of the underlying NNT model describing pure-DNA melting thermodynamics.

The standard SBT model utilizes a set of $\Delta\Delta S_i^o$ parameters, each of which is specific to the base pair in which the LNA of type i is present. It, therefore, can be used to show that the incremental contribution to duplex stability of an internal LNA:DNA base pair (relative to the DNA:DNA base pair from which it is derived) is the same irrespective of whether the LNA:DNA base pair is flanked by DNA:DNA base pairs or by one or more LNA:DNA base pairs. At present, this additive effect, which is foundational to group-contribution-type models, has only been demonstrated for the case where all LNA:DNA base pairs are oriented in the same direction. Below, we investigate cases where LNAs are present on both strands, so that LNA:LNA base pairs and/or oppositely oriented LNA:DNA base pairs are formed.

Library design for analyzing the effect of LNA:LNA base pairs and oppositely oriented LNA:DNA base pairs on duplex stability

Short complementary duplexes were created to study changes in thermal stability arising from an LNA substitution within each strand. Sequence information and LNA content for each duplex are provided in Table 2 along with T_m and complete melting thermodynamic data for the duplex obtained from UV spectroscopy experiments. The general structure of the library is provided in Figure 2 in accordance with the $-4 \le j \le 3$ nomenclature described above. Each duplex having two LNA substitutions contains either a single LNA:LNA base pair ($j = 0$) or two oppositely oriented LNA:DNA base pairs. The library was designed based on pure-DNA duplexes covering a range of *g*/*c* content and base-pair sequences. From these, the set of LNA-substituted duplexes was created so as to provide complete coverage and excellent redundancy in the types of LNA:LNA and oppositely oriented LNA:DNA base pairs formed, as well as in the types of base pairs neighboring and between each of those LNA-containing base pairs.

Most of the duplex sequences used were selected from literature as they had previously been shown to exhibit two-state melting behavior. However, four duplexes, which likewise exhibit two-state melting behavior based on repeated UV melt experiments, were designed using Exiqon's (Vedbaek, Denmark) LNA Oligo Optimizer tool software to preclude formation of secondary structures (hairpins, homodimers) or slipped duplex structures. LNA substitutions within either terminal nearest-neighbor base pair were excluded so as to avoid unwanted edge-effect (e.g., duplex fraying) contributions to regressed $\Delta\Delta G^{\mathrm{o}}_{\mathrm{hyper}-(j)}$ parameters.

The incremental stability of an LNA:LNA base pair exceeds the summed incremental stabilities of the two LNA:DNA base pairs from which it is derived

Our library of duplexes containing an LNA substitution within each strand (Table 2) includes 15 duplexes where the LNAs align to form a single LNA:LNA base pair (i.e., the $j = 0$ case). For each, the library also includes (see Table 1) two single-LNA-substituted duplexes of the same sequence, each of which bears one of the two parent LNA:DNA base pairs from which the LNA:LNA base pair can form via a second LNA substitution. The library likewise includes the unsubstituted pure-DNA isosequence, which completes a set of four duplexes of the same sequence but of varying LNA

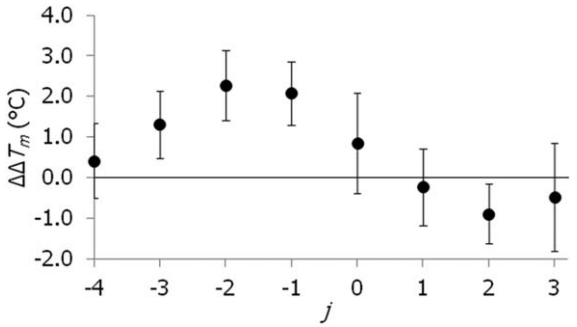

Figure 3. Hyperstabilization of duplexes containing a single LNA substitution on each strand defined in terms of $\Delta\Delta T_{m,\mathrm{LNA}}$ (see Eq. 20); the value of index *j* is as defined in Figure 2.

A $\Delta\Delta T_{m,LNA}$ positive in value indicates that the specific spacing of oppositely oriented LNA:DNA base pairs hyperstabilizes the duplex relative to the sum of the incremental stability enhancements provided by each LNA:DNA base pair alone.

content at the $j = 0$ position. Melting thermodynamic data were collected for the 15 such sets of sequence-related duplexes so as to parse out the incremental contribution of an LNA:LNA base pair to duplex stability, including its relation to the stabilities of the two duplexes bearing one of the parent LNA:DNA base pairs. Taking the Gibbs energy change for melting of the isosequential pure-DNA duplex $\Delta G^{\circ}_{\mathrm{DNA}}$ at $\mathrm{T_{ref}}$ (53°C) as a reference, the incremental enhancement to duplex stability ($\Delta\Delta G^{\circ}_{\mathrm{LNA:LNA-0}}$) provided by the replacement of an internal DNA:DNA base pair with its corresponding LNA:LNA base pair is given at T_{ref} by

$$\Delta\Delta G^{\circ}_{\mathrm{LNA:LNA-0}} = \Delta G^{\circ}_{\mathrm{LNA}} - \Delta G^{\circ}_{\mathrm{DNA}} \tag{16}$$

As the standard SBT model accounts for the energetics of LNA:DNA base pairs, it can be most easily extended to permit prediction of melting thermodynamics for duplexes bearing an LNA:LNA base pair by expressing $\Delta\Delta G^{\circ}_{LNA:LNA-0}$ as

$$\Delta\Delta G^{\circ}_{\mathrm{LNA:LNA-0}} = \Delta\Delta G^{\circ}_{\mathrm{LNA:DNA}} + \Delta\Delta G^{\circ}_{\mathrm{DNA:LNA}} + \Delta\Delta G^{\circ}_{\mathrm{hyper-(0)}} \tag{17}$$

where

$$\Delta\Delta G^{\circ}_{\mathrm{LNA:DNA}} = \Delta G^{\circ}_{\mathrm{LNA:DNA}}(T_{\mathrm{ref}}) - \Delta G^{\circ}_{\mathrm{DNA}}(T_{\mathrm{ref}}) \tag{18}$$

and

$$\Delta\Delta G^{\circ}_{\mathrm{DNA:LNA}} = \Delta G^{\circ}_{\mathrm{DNA:LNA}}(T_{\mathrm{ref}}) - \Delta G^{\circ}_{\mathrm{DNA}}(T_{\mathrm{ref}}) \tag{19}$$

In Eq. 17, $\Delta G^{\circ}_{\mathrm{LNA:DNA}}$ and $\Delta G^{\circ}_{\mathrm{DNA:LNA}}$ are defined at T_{ref} and are computed using the standard SBT model and the relation $\Delta G^{\circ} = \Delta H^{\circ} - T_{\mathrm{ref}}\Delta S^{\circ}$; $\Delta\Delta G^{\circ}_{\mathrm{LNA:DNA}}$ and $\Delta\Delta G^{\circ}_{\mathrm{DNA:LNA}}$ represent the change in the Gibbs energy of melting (relative to that of the isosequential pure-DNA duplex) due to a single LNA substitution in the sense or anti-sense strand, respectively. $\Delta\Delta G^{\circ}_{\mathrm{hyper-(0)}}$ then quantifies excess contributions to the stability enhancement provided by the LNA:LNA base pair that are not captured by the sum of the incremental stabilities of the parent LNA:DNA base pairs from which it is derived.

Analyzing the melting thermodynamics data for the learning set, we find that $\Delta\Delta G^{\circ}_{\mathrm{hyper-(0)}} = 0.20 \pm 0.35$ kcal mol^{-1}, and that its value, within experimental error, is not sensitive to either the type of LNA:LNA base pair formed (*A*:*T* or *C*:*G*) or the type of DNA:DNA base pairs neighboring it. Thus, although its error is somewhat larger than desired, $\Delta\Delta G^{\circ}_{\mathrm{hyper-(0)}}$ is small, positive, and constant in value, indicating that the incremental stability of an LNA:LNA base pair exceeds that predicted by the summed incremental stabilities of the parent LNA:DNA base pairs.

A representative example of this effect is provided in Table 3, which reports melting thermodynamic data for a set of duplexes having the pure-DNA 12-mer sequence 5′-*ggaacaagatgc*-3′ and varying LNA content. This pure-DNA duplex, hereafter identified as duplex 10, melts at 54.6°C (at $C_T = 5$ μM). From it, we created three duplexes containing a single LNA substitution in the sense strand; when melted at the same C_T, each has an enhanced stability relative to the isosequential pure-DNA duplex as reflected in the positive ΔT_m value reported. Likewise, the three duplexes having a single LNA in the antisense strand all exhibit a positive ΔT_m. Now, consider the duplex 10-S-L6:AS-L7 containing a single LNA:LNA base pair that is formed from strands S-L6 (where "S" indicates the sense strand, and L6 indicates an LNA substitution at the 5′+6 position of that strand) and AS-L7 (where "AS" indicates the antisense strand). The T_m of this duplex is 62.3°C, giving a ΔT_m of 7.7°C relative to the pure-DNA duplex. Application of Eq. 7 then yields a $\Delta\Delta T_m$ of $\sim$ 2°C (due to the fact that the sum $\Delta T_{m,\text{10-S-L6:AS}} + \Delta T_{m,\text{10-S:AS-L7}} = 5.7$°C), illustrating the hyperstabilizing effect of an LNA:LNA base pair.

5′-Offset oppositely oriented LNA:DNA base pairs also hyperstabilize an LNA-substituted duplex

Inclusion in the library of duplexes in which an LNA substitution on the sense strand is either 5′ or 3′ offset relative to an LNA on the antisense strand permitted measurement of ΔT_m and $\Delta\Delta T_m$ values for duplexes bearing oppositely oriented LNA:DNA base pairs of type *j*. Figure 3 shows that hyperstabilization of duplexes containing a single LNA substitution on each strand occurs for certain arrangements of oppositely oriented LNA:DNA base pairs, such that $\Delta T_{m,\mathrm{LNA}}$ $\left(= T_{m,\mathrm{LNA}} - T_{m,\mathrm{DNA}}\right)$ exceeds $\Delta T_{m,\mathrm{LNA:DNA}} + \Delta T_{m,\mathrm{DNA:LNA}}$ by an amount $\Delta\Delta T_{m,\mathrm{LNA}}$ given by Eq. 7. In particular, statistically significant hyperstabilization of duplexes is observed when the LNA on the antisense strand lies in a position $-3 \le j \le -1$. The average magnitude of the observed hyperstabilization depends on the separation distance between the two oppositely oriented LNA:DNA base pairs, with a maximum stability enhancement observed when the base pairs are 5′ offset and either directly adjacent to one another ($j = -1$), as illustrated by the $\Delta\Delta T_m$ values for duplexes 10-S-L7:AS-L5 and 10-S-

Table 4. $\Delta\Delta G^{\circ}_{\mathbf{hyper\text{-}(j)}}$ Parameters and Their Respective Standard Deviations When Regressed to Either the "Learning Set" (Table 2) Alone, or the Combined "Learning Set" and "Testing Set" (Tables 2 and 5)

LNA Substitution Pattern *j*	$\Delta\Delta G^{\circ}_{\mathrm{hyper\text{-}(j)}}$ (kcal mol^{-1})	
	Learning Set	Whole Dataset
−4	0.01 ± 0.19	0.10 ± 0.25
−3	0.32 ± 0.25	0.35 ± 0.22
−2	0.67 ± 0.25	0.64 ± 0.19
−1	0.54 ± 0.25	0.54 ± 0.20
0	0.20 ± 0.35	0.22 ± 0.32
1	−0.11 ± 0.23	−0.06 ± 0.24
2	−0.22 ± 0.21	−0.23 ± 0.19
3	−0.18 ± 0.36	−0.12 ± 0.35

DOI 10.1002/aic Published on behalf of the AIChE September 2015 Vol. 61, No. 9 AIChE Journal

Table 5. Melting Thermodynamic Data Collected by UV Spectroscopy for the "Testing Set" of Complementary Duplexes Bearing an LNA Substitution on One or Both Strands

	Sense Strand	Antisense Strand							
Duplex Name	(5′-3′)	(5′-3′)	ΔH (kcal mol^{-1})	ΔS (cal mol^{-1} K^{-1})	ΔG^o (kcal mol^{-1})	$\Delta\Delta G^o$ (kcal mol^{-1})	T_m (°C)	ΔT_m (°C)	$\Delta\Delta T_m$ (°C)
8-S-L4:AS-L7	*ggaCctcgac*	*gtcgagGtcc*	79.5 ± 2.1	207.7 ± 5.9	11.70 ± 0.14 (11.05)	2.85 ± 0.22	65.7 ± 0.3 (62.7)	12.6 ± 0.8 (10.0)	1.2 (0.9)
8-S-L5:AS-L6	*ggacCtcgac*	*gtcgaGgtcc*	75.4 ± 1.0	195.1 ± 2.7	11.61 ± 0.07 (11.05)	2.77 ± 0.19	66.1 ± 0.2 (62.7)	12.9 ± 0.8 (10.0)	1.4 (0.9)
8-S-L5:AS-L5	*ggacCtcgac*	*gtcgAggtcc*	77.8 ± 2.5	202.2 ± 7.3	11.71 ± 0.15 (11.12)	2.86 ± 0.23	66.1 ± 0.2 (62.9)	13 ± 0.8 (10.2)	2.0 (2.3)
8-S-L4:AS-L6	*ggaCctcgac*	*gtcgaGgtcc*	76.7 ± 4.2	197.8 ± 12.0	12.00 ± 0.25 (11.38)	3.15 ± 0.30	67.8 ± 0.4 (64.0)	14.6 ± 0.9 (11.3)	0.9 (2.3)
8-S-L7:AS-L5	*ggacctCgac*	*gtcgAggtcc*	84.0 ± 0.8	221.6 ± 2.5	11.66 ± 0.03 (10.51)	2.81 ± 0.18	64.8 ± 0.2 (60.3)	11.6 ± 0.8 (7.6)	0.6 (−0.2)
8-S-L5:AS-L7	*ggacCtcgac*	*gtcgagGtcc*	79.2 ± 4.1	210.0 ± 11.9	10.71 ± 0.16 (10.77)	1.87 ± 0.24	61.2 ± 0.3 (61.5)	8.0 ± 0.8 (8.8)	−1.2 (−0.2)
9-S-L7:AS-L4	*cctgcgAtgac*	*gtcAtcgcagg*	88.7 ± 1.3	236.4 ± 3.6	11.55 ± 0.08 (11.55)	1.66 ± 0.12	63.7 ± 0.2 (63.4)	6.3 ± 0.3 (6.8)	2.1 (2.0)
9-S-L6:AS-L5	*cctgcGatgac*	*gtcaTcgcagg*	85.5 ± 0.8	225.1 ± 2.2	11.92 ± 0.05 (12.13)	2.03 ± 0.10	65.8 ± 0.1 (65.7)	8.4 ± 0.2 (9.1)	2.1 (2.0)
9-S-L8:AS-L3	*cctgcgaTgac*	*gtCatcgcagg*	96.5 ± 1.8	254.7 ± 5.3	13.21 ± 0.06 (12.45)	3.31 ± 0.11	69.3 ± 0.1 (67.0)	11.8 ± 0.2 (10.3)	2.9 (2.0)
9-S-L4:AS-L7	*cctGcgatgac*	*gtcatcGcagg*	85.3 ± 0.4	227.3 ± 1.2	11.14 ± 0.04 (12.07)	1.25 ± 0.10	62.4 ± 0.1 (65.5)	5.0 ± 0.3 (8.8)	2.4 (2.0)
9-S-L5:AS-L6	*cctgCgatgac*	*gtcatCgcagg*	85.8 ± 0.8	223.6 ± 2.4	12.66 ± 0.05 (12.73)	2.77 ± 0.11	69.1 ± 0.1 (68.0)	11.7 ± 0.3 (11.3)	2.5 (2.0)
9-S-L3:AS-L7	*ccTgcgatgac*	*gtcatcGcagg*	88.2 ± 3.8	234.3 ± 11.3	11.67 ± 0.11 (12.22)	1.78 ± 0.14	64.3 ± 0.1 (66.1)	6.9 ± 0.2 (9.4)	2.3 (2.4)
9-S-L4:AS-L6	*cctGcgatgac*	*gtcatCgcagg*	88.9 ± 1.0	235.7 ± 3.0	11.94 ± 0.05 (12.50)	2.05 ± 0.10	65.3 ± 0.1 (67.1)	7.9 ± 0.2 (10.4)	2.2 (2.4)
9-S-L5:AS-L5	*cctgCgatgac*	*gtcaTcgcagg*	88.7 ± 0.2	233.1 ± 0.7	12.52 ± 0.02 (12.55)	2.62 ± 0.09	67.8 ± 0.0 (67.3)	10.4 ± 0.2 (10.7)	2.0 (2.4)
9-S-L6:AS-L4	*cctgcGatgac*	*gtcAtcgcagg*	95.2 ± 1.8	255.1 ± 5.3	11.86 ± 0.07 (11.91)	1.97 ± 0.11	64.1 ± 0.0 (64.8)	6.7 ± 0.2 (8.2)	2.8 (2.4)
9-S-L5:AS-L4	*cctgCgatgac*	*gtcAtcgcagg*	89.1 ± 0.8	236.4 ± 2.3	11.87 ± 0.04 (11.94)	1.98 ± 0.10	65.0 ± 0.1 (65.0)	7.6 ± 0.2 (8.4)	1.5 (1.3)
9-S-L4:AS-L5	*cctGcgatgac*	*gtcaTcgcagg*	95.0 ± 1.8	255.2 ± 5.3	11.69 ± 0.05 (11.93)	1.80 ± 0.10	63.5 ± 0.1 (65.0)	6.1 ± 0.2 (8.4)	1.1 (1.3)
9-S-L6:AS-L3	*cctgcGatgac*	*gtCatcgcagg*	95.9 ± 1.8	254.9 ± 5.3	12.66 ± 0.08 (12.20)	2.77 ± 0.12	67.1 ± 0.0 (66.0)	9.7 ± 0.2 (9.4)	2.5 (1.3)
9-S-L3:AS-L6	*ccTgcgatgac*	*gtcatCgcagg*	88.5 ± 3.8	234.1 ± 11.3	12.06 ± 0.14 (12.25)	2.17 ± 0.17	65.9 ± 0.0 (66.3)	8.5 ± 0.2 (9.6)	0.8 (1.3)
10-S-L7:AS-L6	*ggaacaAgatgc*	*gcatcTtgttcc*	91.2 ± 4.4	245.9 ± 13.0	10.91 ± 0.16 (11.13)	1.68 ± 0.20	60.9 ± 0.3 (61.4)	6.3 ± 0.5 (6.5)	0.2 (0.8)
10-S-L6:AS-L7	*ggaacAagatgc*	*gcatctTgttcc*	89.8 ± 3.4	240.8 ± 10.1	11.22 ± 0.12 (11.13)	1.99 ± 0.17	62.3 ± 0.1 (61.4)	7.7 ± 0.5 (6.5)	1.9 (0.8)
10-S-L7:AS-L5	*ggaacaAgatgc*	*gcatCttgttcc*	94.9 ± 1.5	253.9 ± 4.3	11.95 ± 0.07 (11.73)	2.72 ± 0.14	64.5 ± 0.1 (63.5)	10.0 ± 0.5 (8.5)	1.5 (1.9)

TABLE 5. *Continued*

Duplex Name	Sense Strand (5′-3′)	Antisense Strand (5′-3′)	ΔH (kcal mol^{-1})	ΔS (cal mol^{-1} K^{-1})	ΔG^o (kcal mol^{-1})	$\Delta\Delta G^o$ (kcal mol^{-1})	T_m (°C)	ΔT_m (°C)	$\Delta\Delta T_m$ (°C)
10-S-L6:AS-L6	*ggaacAagatgc*	*gcatcTtgttcc*	93.6 ± 2.3	253.1 ± 6.7	11.00 ± 0.08 (11.46)	1.77 ± 0.14	61.0 ± 0.1 (62.5)	6.4 ± 0.5 (7.6)	2.3 (1.9)
10-S-L4:AS-L8	*ggaAcaagatgc*	*gcatcttGttcc*	97.1 ± 1.2	262.6 ± 3.6	11.42 ± 0.04 (11.40)	2.19 ± 0.12	62.2 ± 0.1 (62.3)	7.7 ± 0.5 (7.3)	2.3 (1.9)
10-S-L4:AS-L7	*ggaAcaagatgc*	*gcatctTgttcc*	91.1 ± 1.5	244.0 ± 4.3	11.44 ± 0.06 (11.55)	2.21 ± 0.13	63.0 ± 0.1 (62.9)	8.4 ± 0.5 (7.9)	2.3 (2.3)
10-S-L6:AS-L5	*ggaacAagatgc*	*gcatCttgttcc*	90.2 ± 3.1	241.3 ± 9.2	11.46 ± 0.13 (11.83)	2.23 ± 0.17	63.2 ± 0.1 (63.8)	8.6 ± 0.5 (8.9)	2.2 (2.26)
10-S-L4:AS-L6	*ggaAcaagatgc*	*gcatcTtgttcc*	89.9 ± 1.9	242.8 ± 5.6	10.71 ± 0.05 (11.26)	1.48 ± 0.13	60.2 ± 0.0 (61.9)	5.6 ± 0.5 (6.9)	1.2 (1.2)
10-S-L4:AS-L5	*ggaAcaagatgc*	*gcatCttgttcc*	94.5 ± 1.2	254.3 ± 3.7	11.47 ± 0.05 (11.28)	2.24 ± 0.13	62.7 ± 0.1 (61.9)	8.2 ± 0.5 (7.0)	1.4 (0.4)
10-S-L6:AS-L8	*ggaacAagatgc*	*gcatcttGttcc*	91.5 ± 4.9	246.9 ± 14.3	10.91 ± 0.18 (10.80)	1.68 ± 0.22	60.8 ± 0.3 (60.2)	6.3 ± 0.5 (5.2)	1.2 (−0.2)
10-S-L7:AS-L7	*ggaacaAgatgc*	*gcatctTgttcc*	93.6 ± 1.7	251.3 ± 5.2	11.55 ± 0.06 (10.85)	2.32 ± 0.13	63.1 ± 0.1 (60.4)	8.6 ± 0.5 (5.5)	0.7 (−0.2)
10-S-L9:AS-L5	*ggaacaagAtgc*	*gcatCttgttcc*	87.3 ± 3.5	233.4 ± 10.3	11.06 ± 0.12 (11.12)	1.83 ± 0.17	61.9 ± 0.1 (61.4)	7.3 ± 0.5 (6.4)	−0.3 (−0.2)
10-S-L9:AS-L6	*ggaacaagAtgc*	*gcatcTtgttcc*	92.2 ± 1.6	250.8 ± 4.6	10.43 ± 0.07 (10.68)	1.20 ± 0.14	58.9 ± 0.2 (59.8)	4.4 ± 0.5 (4.9)	−0.9 (−0.8)
10-S-L7:AS-L8	*ggaacaAgatgc*	*gcatcttGttcc*	96.9 ± 1.8	263.6 ± 5.5	10.94 ± 0.05 (10.63)	1.71 ± 0.13	60.5 ± 0.1 (59.6)	5.9 ± 0.5 (4.6)	−1.2 (−0.8)
10-S-L9:AS-L7	*ggaacaagAtgc*	*gcatctTgttcc*	93.3 ± 1.3	251.3 ± 3.7	11.26 ± 0.06 (10.79)	2.03 ± 0.13	62.0 ± 0.1 (60.2)	7.5 ± 0.5 (5.2)	0.5 (−0.4)
11-S-L12:AS-L4	*acgaccagagtTacag*	*ctgTaactctggtcgt*	115.1 ± 1.8	304.2 ± 5.1	15.41 ± 0.10 (15.95)	1.87 ± 0.15	74.3 ± 0.0 (72.2)	6.9 ± 0.1 (6.5)	1.2 (1.4)
11-S-L11:AS-L4	*acgaccagagTtacag*	*ctgTaactctggtcgt*	113.8 ± 0.9	301.3 ± 2.7	15.13 ± 0.05 (16.05)	1.60 ± 0.12	73.5 ± 0.1 (72.4)	6.2 ± 0.1 (6.8)	1.0 (1.6)
11-S-L9:AS-L6	*acgaccagAgttacag*	*ctgtaActctggtcgt*	110.6 ± 0.5	290.5 ± 1.3	15.36 ± 0.04 (15.42)	1.82 ± 0.11	75.2 ± 0.1 (70.7)	7.8 ± 0.1 (5.0)	1.2 (1.6)
11-S-L3:AS-L12	*acGaccagagttacag*	*ctgtaactctgGtcgt*	114.7 ± 0.6	304.8 ± 1.7	14.90 ± 0.03 (15.94)	1.36 ± 0.11	72.5 ± 0.1 (72.1)	5.2 ± 0.1 (6.4)	1.5 (1.6)
11-S-L6:AS-L9	*acgacCagagttacag*	*ctgtaactCtggtcgt*	112.1 ± 0.7	294.6 ± 2.0	15.53 ± 0.03 (16.59)	2.00 ± 0.11	75.5 ± 0.1 (73.8)	8.1 ± 0.1 (8.2)	1.5 (1.6)
11-S-L9:AS-L4	*acgaccagAgttacag*	*ctgtAactctggtcgt*	110.6 ± 0.5	291.2 ± 1.6	15.19 ± 0.03 (15.12)	1.65 ± 0.11	74.5 ± 0.1 (69.9)	7.1 ± 0.1 (4.3)	1.7 (0.9)
11-S-L3:AS-L11	*acGaccagagttacag*	*ctgtaactctGgtcgt*	117.7 ± 1.5	312.8 ± 4.2	15.30 ± 0.08 (15.97)	1.77 ± 0.14	73.3 ± 0.0 (71.3)	6.0 ± 0.1 (5.7)	1.6 (0.9)
11-S-L5:AS-L9	*acgaCcagagttacag*	*ctgtaactCtggtcgt*	112.2 ± 1.3	294.4 ± 3.8	15.62 ± 0.09 (16.30)	2.08 ± 0.14	75.8 ± 0.1 (73.1)	8.4 ± 0.1 (7.4)	0.9 (0.9)

Values reported in parentheses are the corresponding melting thermodynamics predicted by the extended SBT model. The reported UVM data ($\Delta H(T_m)$, $\Delta S(T_m)$, $\Delta G°$, and T_m) are for the helix-to-coil transition and were determined as reported in Materials and Methods. The reported errors refer to the standard deviation of triplicate runs. All duplex samples were resuspended in buffer containing 1 M NaCl, 10 mM Na_2HPO_4, and 1 mM Na_2EDTA (pH = 7.0) to a $C_T = 5$ μM.

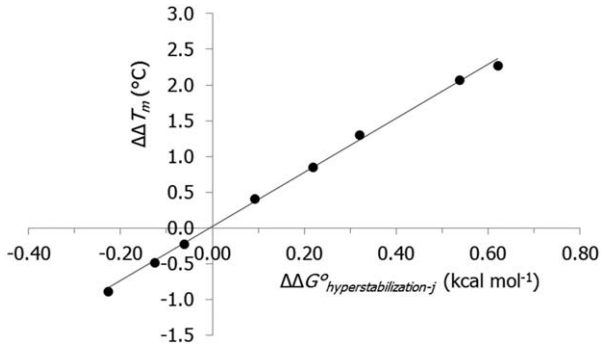

Figure 4. $\Delta\Delta T_m$ depends linearly on $\Delta\Delta G^o_{\text{hyper-}(j)}$ (whole dataset derived model parameters in Table 4) as required by Eq. 10.

L6:AS-L6 (Table 3), or separated by a single DNA:DNA base pair ($j = -2$).

Interestingly, we find conversely that 3′ off-setting of oppositely oriented LNA-DNA base pairs is slightly destabilizing (relative to the summed incremental stabilities of the parent LNA:DNA base pairs) for the specific case of $j = 2$.

Our proposed extension (i.e., Eq. 13) to the SBT model assumes that the total hyperstabilization of a duplex bearing multiple LNA substitutions in each strand may be computed as a frequency weighted sum of $\Delta\Delta G^{\circ}_{\text{hyper}-(j)}$; in turn, we will later show that $\Delta\Delta T_{m,j}$ for a duplex bearing a pair of LNAs on each strand of type j orientation is linearly proportional to $\Delta\Delta G^{\circ}_{\text{hyper}-(j)}$. As a result, the measured total $\Delta\Delta T_m$ for a duplex bearing multiple LNAs on each strand is equal to the sum of the frquency weighted $\Delta\Delta T_{m,j}$

$$\Delta\Delta T_m = \sum n_j \Delta\Delta T_{m,j} \tag{20}$$

This is illustrated for both the 10-S-L79:AS-L5 duplex, which bears oppositely oriented LNA:DNA base pairs of type $j = 1$ and $j = -1$, and the 10-S-L6:AS-L67 duplex, which bears a single $j = 0$ and a single $j = -1$ type LNA-substitution pattern. For duplex 10-S-L79:AS-L5, $\Delta\Delta T_m = 1.2$°C, which matches the sum of $\Delta\Delta T_{m,j}$ (= 1.5°C + (−0.3°C)). Similar support for Eq. 20 is provided by the 10-S-L6:AS-L67 duplex.

Extending the SBT model to permit application to duplexes containing LNA substitutions on both strands

The illustrative results reported above indicate that the standard SBT model may be extended as defined in Eqs. 10–13 to model duplexes containing combinations of LNA:LNA base pairs and offset LNA:DNA base pairs. Extension of the model requires a set of $\Delta\Delta G^{\circ}_{\text{hyper}-(j)}$ parameters. Those parameters were determined by globally fitting Eqs. 10–13 to the collective melting thermodynamic data for the "learning set" (Table 2). The regressed $\Delta\Delta G^{\circ}_{\text{hyper}-(j)}$ are reported in Table 4 along with their respective standard deviations. In accordance with Figure 3, statistically significant $\Delta\Delta G^{\circ}_{\text{hyper}-(j)}$ parameters were obtained for LNA substitution patterns on opposite strands corresponding to $j = -3$ to -1, as well as to $j = 2$ (small destabilizing effect). As observed with the $\Delta\Delta G^{\circ}_{\text{hyper}-(0)}$ parameter, we find that the value of each $\Delta\Delta G^{\circ}_{\text{hyper}-(j)}$ is insensitive to both the types of LNAs substituted and the types of neighboring base pairs, at least within the error of our experimental data. In addition, and more importantly, we indeed find that the total hyperstabilization of a duplex containing multiple substitution patterns in each strand is given by the linear addition of frequency-weighted $\Delta\Delta G^{\circ}_{\text{hyper}-(j)}$, allowing the classic group-contribution method embodied in Eq. 13 to be applied to duplexes having dual-strand patterns of LNA substitutions. Two exceptions are noted. The first is that no hyperstablization effect is applied to any LNA substitutions at either terminus, as both our lab[19] and others[50,51] have demonstrated that LNA substitutions made to either the 5′ or 3′ termini provide little to no additional stability to the duplex. The second applies to internal tandem (directly adjacent) LNA:LNA base pairs, which have not been investigated here and for which the extended SBT model, therefore, cannot be applied. Preliminary melting data acquired in our laboratory suggest that the tandem LNA:LNA motif strongly hyperstabilizes a duplex, but the precise magnitude and nature of this effect remains an open question that is currently under study.

Table 5 reports melting thermodynamics collected by UV spectroscopy for a "testing set" of complementary duplexes bearing various levels and patterns of LNA substitutions. In general, users of models designed to predict melting thermodynamics of either pure-DNA duplexes or LNA-substituted duplexes are primarily interested in the prediction of T_m, as well as ΔT_m and $\Delta\Delta T_m$ to a lesser extent, because that information is essential to the design of primers, probes, and gene-silencing agents. Thus, for each duplex within the testing set, T_m, ΔT_m, and $\Delta\Delta T_m$ values predicted by the extended SBT model are also reported (in parentheses) in Table 5. Table 6 then summarizes the overall melting-temperature prediction performance of the extended SBT model when sequentially applied to the learning set, testing set, and full set of duplex sequences reported in Tables 2 and 5. As one might expect, excellent performance is observed when the model is applied to the "learning set" sequences whose melting thermodynamics were collectively used to regress extended model parameters. The NNT model,[41] on which both the standard and extended SBT model are based, predicts T_m values for pure-DNA duplexes with a mean error ± standard deviation of -0.2 ± 1.4°C. The fact that a comparable overall error is found for the extended SBT model in predicting T_m values for duplexes containing various LNA substitution patterns suggests that the proposed group-contribution approach to modeling the stabilizing and hyperstabilizing effects of LNAs is not only sound, but highly accurate. This is particularly true of the hyperstabilization effects, which were the central concern in this work; indeed, the overall error in predicted $\Delta\Delta T_m$ values (see Eq. 7) is 0.0 ± 1.0°C when applied to the learning set.

Extended SBT model performance remains very good when applied to the prediction of T_m, ΔT_m, and $\Delta\Delta T_m$ values for all "testing set" duplexes containing LNAs in both strands, with the model again showing a near zero mean error in $\Delta\Delta T_m$. Of greatest importance here is the fact that through use of the group-contribution approach embodied in Eq. 13, the extended SBT model accurately captures all hyperstabilization effects,

Table 6. Summary of Overall Prediction Performance of the Extended SBT Model ("Learning Set" Regressed $\Delta\Delta G^{\circ}_{\text{hyper-}(j)}$ Parameters) When Sequentially Applied to the Learning Set, Testing Set, and Combined Set of Duplex Sequences Reported in Tables 2 and 5

Dataset	T_m (°C)	ΔT_m (°C)	$\Delta\Delta T_m$ (°C)
Learning	-0.7 ± 1.3	-0.3 ± 1.3	0.0 ± 1.0
Testing	-0.9 ± 1.9	-0.4 ± 1.8	-0.2 ± 0.7
Overall	-0.8 ± 1.5	-0.3 ± 1.5	-0.1 ± 0.9

Table 7. Performance of the Extended SBT Model When Applied to a Set of Duplexes Bearing Various LNA-Substitution Patterns in Both Strands[a]

Duplex Name	Sense Strand (5′-3′)	Antisense Strand (5′-3′)	T_m (°C)	ΔT_m (°C)	$\Delta\Delta T_m$ (°C)
8-S-L57:AS-L5	*ggacCtCgac*	*gtcgAggtcc*	72.5 ± 0.4	19.3 ± 0.9	2.4
			(67.8)	(15.0)	(2.0)
8-S-L5:AS-L67	*ggacCtcgac*	*gtcgaGGtcc*	68.9 ± 0.3	15.7 ± 0.8	0.8
			(66.2)	(13.4)	(0.7)
8-S-L4:AS-L67	*ggaCctcgac*	*gtcgaGGtcc*	72.4 ± 0.3	19.2 ± 0.8	2.1
			(68.7)	(15.9)	(3.2)
8-S-L45:AS-L6	*ggaCCtcgac*	*gtcgaGgtcc*	72.5 ± 1.0	19.3 ± 1.2	3.4
			(70.1)	(17.3)	(3.2)
8-S-L45:AS-L7	*ggaCCtcgac*	*gtcgagGtcc*	67.5 ± 0.4	14.4 ± 0.9	0.8
			(67.6)	(14.8)	(0.7)
8-S-L57:AS-L67	*ggacCtCgac*	*gtcgaGGtcc*	74.8 ± 0.5	21.6 ± 0.9	0.7
			(70.0)	(17.2)	(−0.7)
10-S-L7:AS-L67	*ggaacaAgatgc*	*gcatcTTgttcc*	66.5 ± 0.1	11.9 ± 0.5	1.4
			(67.5)	(12.5)	(1.6)
10-S-L6:AS-L67	*ggaacAagatgc*	*gcatcTTgttcc*	66.7 ± 0.0	12.1 ± 0.5	3.7
			(66.7)	(11.6)	(2.7)
10-S-L67:AS-L6	*ggaacAAgatgc*	*gcatcTtgttcc*	66.3 ± 0.1	11.7 ± 0.5	4.2
			(65.5)	(10.5)	(2.7)
10-S-L67:AS-L7	*ggaacAAgatgc*	*gcatctTgttcc*	65.3 ± 0.1	10.8 ± 0.5	1.5
			(66.4)	(11.3)	(1.6)
10-S-L46:AS-L8	*ggaAcAagatgc*	*gcatcttGttcc*	65.7 ± 0.1	11.1 ± 0.5	2.0
			(64.3)	(9.3)	(1.7)
10-S-L79:AS-L5	*ggaacaAgAtgc*	*gcatCttgttcc*	67.6 ± 0.3	13.0 ± 0.5	1.2
			(65.5)	(10.5)	(1.1)
10-S-L79:AS-L67	*ggaacaAgAtgc*	*gcatcTTgttcc*	70.1 ± 0.2	15.5 ± 0.5	1.7
			(68.5)	(12.5)	(0.7)
10-S-L79:AS-L8	*ggaacaAgAtgc*	*gcatcttGttcc*	64.5 ± 0.0	9.9 ± 0.5	−0.5
			(64.8)	(8.8)	(−0.8)
10-S-L67:AS-L8	*ggaacAAgatgc*	*gcatcttGttcc*	63.9 ± 0.2	9.4 ± 0.5	0.9
			(61.6)	(7.6)	(−1.0)
10-S-L67:AS-L5	*ggaacAAgatgc*	*gcatCttgttcc*	68.6 ± 0.1	14.0 ± 0.5	4.2
			(69.0)	(13.9)	(4.1)
10-S-L46:AS-L67	*ggaAcAagatgc*	*gcatcTTgttcc*	74.4 ± 0.0	19.8 ± 0.5	7.2
			(74.3)	(17.2)	(7.1)

[a]Melting thermodynamic data reported above were collected by UV spectroscopy at a $C_T = 5$ μM in buffer containing 1 M NaCl, 10 mM Na_2HPO_4, and 1 mM Na_2EDTA (pH = 7.0).

which can be significant. For the 10-S-L6:AS-L67 duplex (Table 1), for example, hyperstabilization effects contribute 3.7°C (31%) of the 12.1°C increase in duplex T_m arising from the LNA substitutions.

The stability of the hyperstabilization parameters was then evaluated through their re-regression to the entire dataset (i.e., "learning set" + "testing set"), and the resulting whole-dataset derived parameters are also reported in Table 4. For those parameters that are statistically significant ($-3 \le j \le -1$, $j = 2$), the two sets of regressed values are essentially identical, indicating a lack of end-effect or other error sources in the "learning set" that might serve to bias parameter estimates. Moreover, for either dataset, $\Delta\Delta T_m$ is found to depend linearly on $\Delta\Delta G^{o}_{hyper}$, as required by Eq. 10 and as shown in Figure 4 for the whole-dataset derived parameters.

As a final test, we applied the extended SBT model (w/ whole-dataset derived parameters) to a small set of duplexes bearing more complex LNA-substitution patterns in both strands, with a comparison of predicted and experimental melting thermodynamics provided in Table 7. The results show that the extended SBT model predicts well melting thermodynamics for duplexes bearing more complex combinations of both LNA:LNA and oppositely oriented LNA:DNA base pairs, exibiting errors of -1.3 ± 1.5°C, -0.8 ± 1.4°C, and -0.3 ± 0.7°C for T_m, ΔT_m, and $\Delta\Delta T_m$, respectively. At present, no other model is designed or able to make such predictions. As an extreme test of the model, we also used the model to predict $\Delta\Delta T_m$ for a highly substituted duplex, of sequence S-L257:AS-L358 using our nomenclature, which Koshkin et al.[6] reported melts at a T_m 34°C higher than that for the corresponding isosequential pure-DNA duplex. The hyperstabilization effect, quantified as $\Delta\Delta T_m$, accounts for about 23% of that dramatic increase in T_m and the extended SBT model predicts a $\Delta\Delta T_m$ of 7.6°C, which is in good agreement with the measured values of 8.0°C.

Concluding Remarks

The unique stabilization properties of LNAs are creating exciting opportunities to generate highly specific therapeutic aptamers exhibiting improved stability and half-life, as well as more potent cell-internalization characteristics, to improve real-time and digital PCR-based detection of rare, clinically important gene mutations, and to create next-generation molecular beacons and related diagnostic probes that show unequivocal specificity for their target. However, fully exploiting LNA technology in these areas will require model-based methods for predicting the hybridization thermodynamics of duplexes bearing complex LNA substitution patterns. The nearest-neighbor SBT model we previously reported accurately predicts melting thermodynamics for both complementary[19] and mismatched[49] DNA duplexes containing any pattern of LNA substitutions in one strand.

Here, we have shown that a group-contribution modeling approach can be used to extend the SBT model to achieve accurate predictions of melting temperatures for short

complementary duplex DNA containing various patterns of LNA substitutions within both strands. It accounts for both the instrinsic stability of an LNA-containing base pair, and hyperstabilization effects created by certain patterns of proximal LNA-containing base pairs. As the hyperstabilization effects are generally subtle, experiment does not permit their associated enthalpic and entropic contributions to be defined in a statistically significant manner. However, for specific patterns of LNA:LNA and oppositely oriented LNA:DNA base pairs, the contribution of hyperstabilization effects can be and therefore is described at the Gibbs energy level. The resulting extended SBT model thereby achieves good prediction of T_m and ΔT_m for duplexes bearing LNAs in both strands; since $\Delta\Delta T_m$ depends linearly on $\Delta\Delta G^{\circ}_{\text{hyper}}$, $\Delta\Delta G^{\circ}_{\text{LNA}}$ values are predicted with equivalent accuracy. ΔH and ΔS are, of course, not treated by the model, which is not of significant concern as models of this type are almost exclusively used by biologists and biotechnologists to predict T_m. It is important to note that all melting thermodynamics reported in this work were collected in a buffer solution containing 1 M NaCl, 10 mM Na_2HPO_4, and 1 mM Na_2EDTA at pH = 7.0. All model predictions reported apply to that standard condition as well. However, excellent, highly accurate methods for converting melting thermodynamics to other solution conditions are available (see Ref. 47 for a review of these methods).

The development of the extended SBT model required the collection of complete melting thermodynamics data for a large set of pure-DNA and LNA-substituted duplexes redundantly covering all possible LNA:LNA base pairs and oppositely oriented LNA:DNA base pairs. Such data, particularly for the latter class of duplexes, have rarely appeared in the literature,[52] making this a valuable contribution that may serve to better understand the molecular nature of the stabilizing properties of LNAs. Evidence for this is provided by our use of the dataset to uncover the general ability of specific patterns of LNA substitutions in opposite strands to hyperstabilize a duplex. At present, the model does not apply to all possible substitution patterns, as it does not address certain motifs such as tandem LNA:LNA base pairs and their hyperstabilizing effect. The study of those motifs is underway, but the results and model presented here constitute a novel and reliable approach to predicting T_m and ΔT_m values for many duplexes for which effective therapeutic or diagnostic use depends on precise LNA substitution patterns and associated thermal stabilities.

Acknowledgments

This work was supported by grants from the Natural Sciences and Engineering Research Council of Canada (NSERC), Canadian Institutes of Health Research (CIHR) and the Michael Smith Development Fund. C. Haynes receives salary support as a Canada Research Chair. He dedicates this work to his friend, mentor and PhD co-supervisor Dr. John Prausnitz, who has provided important ideas, unwavering support and unparalleled inspiration for many greatly appreciated years.

Literature Cited

1. Khakshoor O, Kool ET. Chemistry of nucleic acids: impacts in multiple fields. *Chem Commun (Camb)*. 2011;47(25):7018–7024.
2. Leumann CJ. DNA analogues: from supramolecular principles to biological properties. *Bioorg Med Chem.* 2002;10(4):841–854.
3. Mathé C, Périgaud C. Recent approaches in the synthesis of conformationally restricted nucleoside analogues. *Eur J Org Chem*. 2008; 2008(9):1489–1505.
4. Veedu RN, Wengel J. Locked nucleic acids: promising nucleic acid analogs for therapeutic applications. *Chem Biodivers*. 2010;7(3):536–542.
5. Vester B, Wengel J. LNA (locked nucleic acid): high-affinity targeting of complementary RNA and DNA. *Biochemistry*. 2004;43(42): 13233–13241.
6. Koshkin AA, Nielsen P, Meldgaard M, Rajwanshi VK, Singh SK, Wengel J. LNA (locked nucleic acid): an RNA mimic forming exceedingly stable LNA:LNA duplexes. *J Am Chem Soc*. 1998; 120(50):13252–13253.
7. Obika S, Nanbu D, Hari Y, et al. Stability and structural features of the duplexes containing nucleoside analogues with a fixed N-type conformation, 2′-O,4′-C-methyleneribonucleosides. *Tetrahedron Lett*. 1998;39(30):5401–5404.
8. Obika S, Nanbu D, Hari Y, et al. Synthesis of 2′-O,4′-C-methyleneuridine and -cytidine. Novel bicyclic nucleosides having a fixed C3, -endo sugar puckering. *Tetrahedron Lett*. 1997;38(50):8735–8738.
9. Kaur H, Wengel J, Maiti S. Thermodynamics of DNA-RNA heteroduplex formation: effects of locked nucleic acid nucleotides incorporated into the DNA strand. *Biochemistry*. 2008;47(4):1218–1227.
10. Petersen M, Wengel J. LNA: a versatile tool for therapeutics and genomics. *Trends Biotechnol*. 2003;21(2):74–81.
11. Jakobsen MR, Haasnoot J, Wengel J, Berkhout B, Kjems J. Efficient inhibition of HIV-1 expression by LNA modified antisense oligonucleotides and DNAzymes targeted to functionally selected binding sites. *Retrovirology*. 2007;4:29.
12. Wahlestedt C, Salmi P, Good L, et al. Potent and nontoxic antisense oligonucleotides containing locked nucleic acids. *Proc Natl Acad Sci USA*. 2000;97(10):5633–5638.
13. Karlsen KK, Wengel J. Locked nucleic acid and aptamers. *Nucleic Acid Ther*. 2012;22(6):366–370.
14. Barciszewski J, Medgaard M, Koch T, Kurreck J, Erdmann VA. Locked nucleic acid aptamers. *Methods Mol Biol*. 2009;535: 165–186.
15. Mallikaratchy PR, Ruggiero A, Gardner JR, et al. A multivalent DNA aptamer specific for the B-cell receptor on human lymphoma and leukemia. *Nucleic Acids Res*. 2011;39(6):2458–2469.
16. Ugozzoli LA, Latorra D, Puckett R, Arar K, Hamby K. Real-time genotyping with oligonucleotide probes containing locked nucleic acids. *Anal Biochem*. 2004;324(1):143–152.
17. Warshawsky I, Mularo F. Locked nucleic acid probes for enhanced detection of FLT3 D835/I836, JAK2 V617F and NPM1 mutations. *J Clin Pathol*. 2011;64(10):905–910.
18. Singh P, Mustapha A. Multiplex TaqMan(R) detection of pathogenic and multi-drug resistant Salmonella. *Int J Food Microbiol*. 2013; 166(2):213–218.
19. Hughesman CB, Turner RFB, Haynes CA. Role of the heat capacity change in understanding and modeling melting thermodynamics of complementary duplexes containing standard and nucleobase-modified LNA. *Biochemistry*. 2011;50(23):5354–5368.
20. Kierzek E, Ciesielska A, Pasternak K, Mathews DH, Turner DH, Kierzek R. The influence of locked nucleic acid residues on the thermodynamic properties of 2′-O-methyl RNA/RNA heteroduplexes. *Nucleic Acids Res*. 2005;33(16):5082–5093.
21. McTigue PM, Peterson RJ, Kahn JD. Sequence-dependent thermodynamic parameters for locked nucleic acid (LNA)-DNA duplex formation. *Biochemistry*. 2004;43(18):5388–5405.
22. Owczarzy R, You Y, Groth CL, Tataurov AV. Stability and mismatch discrimination of locked nucleic acid-DNA duplexes. *Biochemistry*. 2011;50(43):9352–9367.
23. Nielsen KE, Singh SK, Wengel J, Jacobsen JP. Solution structure of an LNA hybridized to DNA: NMR study of the d(CT(L)GCT(L)T(L)CT(L)GC):d(GCAGAAGCAG) duplex containing four locked nucleotides. *Bioconjug Chem*. 2000;11(2):228–238.
24. Petersen M, Bondensgaard K, Wengel J, Jacobsen JP. Locked nucleic acid (LNA) recognition of RNA: NMR solution structures of LNA:RNA hybrids. *J Am Chem Soc*. 2002;124(21):5974–5982.
25. Konorov SO, Georg Schulze H, Addison CJ, Haynes CA, Blades MW, Turner RFB. Ultraviolet resonance Raman spectroscopy of locked single-stranded oligo(dA) reveals conformational implications of the locked ribose in LNA. *J Raman Spectrosc*. 2009;40(9):1162–1171.

26. Konorov SO, Schulze HG, Addison CJ, Haynes CA, Blades MW, Turner RFB. Base stacking configuration is a major determinant of excited state dynamics in A−T DNA and LNA. *Open Spectrosc J*. 2009;3:9–20.
27. Konorov SO, Schulze HG, Addison CJ, Haynes CA, Turner RFB, Blades MW. Temperature-dependent excited state absorption in DNA and LNA oligomers supports an emerging model of excited state dynamics in DNA. *Open Spectrosc J*. 2009;3:43–51.
28. Koshkin AA, Singh SK, Nielsen P, et al. LNA (locked nucleic acids): synthesis of the adenine, cytosine, guanine, 5-methylcytosine, thymine and uracil bicyclonucleoside monomers, oligomerisation, and unprecedented nucleic acid recognition. *Tetrahedron*. 1998; 54(14):3607–3630.
29. Singh SK, Koshkin AA, Wengel J, Nielsen P. LNA (locked nucleic acids): synthesis and high-affinity nucleic acid recognition. *Chem Commun*. 1998;(4):455–456.
30. Tolstrup N, Nielsen PS, Kolberg JG, Frankel AM, Vissing H, Kauppinen S. OligoDesign: optimal design of LNA (locked nucleic acid) oligonucleotide capture probes for gene expression profiling. *Nucleic Acids Res*. 2003;31(13):3758–3762.
31. Bruylants G, Boccongelli M, Snoussi K, Bartik K. Comparison of the thermodynamics and base-pair dynamics of a full LNA:DNA duplex and of the isosequential DNA:DNA duplex. *Biochemistry*. 2009;48(35):8473–8482.
32. Fredenslund A, Jones RL, Prausnitz JM. Group-contribution estimation of activity-coefficients in nonideal liquid-mixtures. *AIChE J*. 1975;21(6):1086–1099.
33. Oishi T, Prausnitz JM. Estimation of solvent activities in polymer-solutions using a group-contribution method. *Ind Eng Chem Process Des Dev*. 1978;17(3):333–339.
34. Gmehling J, Li JD, Schiller M. A modified unifac model. 2. Present parameter matrix and results for different thermodynamic properties. *Ind Eng Chem Res*. 1993;32(1):178–193.
35. Larsen BL, Rasmussen P, Fredenslund A. A modified unifac group-contribution model for prediction of phase-equilibria and heats of mixing. *Ind Eng Chem Res*. 1987;26(11):2274–2286.
36. Poland D, Scheraga HA. Occurrence of a phase transition in nucleic acid models. *J Chem Phys*. 1966;45(5):1464–1469.
37. Poland D, Scheraga HA. Phase transitions in one dimension and the helix-coil transition in polyamino acids. *J Chem Phys*. 1966;45(5): 1456–1463.
38. Fisher ME. Effect of excluded volume on phase transitions in biopolymers. *J Chem Phys*. 1966;45(5):1469–1473.
39. Causo MS, Coluzzi B, Grassberger P. Simple model for the DNA denaturation transition. *Phys Rev E Stat Phys Plasmas Fluids Relat Interdiscip Topics*. 2000;62(3 Pt B):3958–3973.
40. SantaLucia J Jr, Hicks D. The thermodynamics of DNA structural motifs. *Annu Rev Biophys Biomol Struct*. 2004;33:415–440.
41. Hughesman CB, Turner RF, Haynes C. Correcting for heat capacity and 5′-TA type terminal nearest neighbors improves prediction of DNA melting temperatures using nearest-neighbor thermodynamic models. *Biochemistry*. 2011;50(13):2642–2649.
42. Mikulecky PJ, Feig AL. Heat capacity changes associated with nucleic acid folding. *Biopolymers*. 2006;82(1):38–58.
43. Wang L, Yang CJ, Medley CD, Benner SA, Tan W. Locked nucleic acid molecular beacons. *J Am Chem Soc*. 2005;127(45):15664–15665.
44. Morandi L, de Biase D, Visani M, et al. Allele specific locked nucleic acid quantitative PCR (ASLNAqPCR): an accurate and cost-effective assay to diagnose and quantify KRAS and BRAF mutation. *PLoS One*. 2012;7(4):e36084.
45. Di Primo C, Rudloff I, Reigadas S, Arzumanov AA, Gait MJ, Toulme JJ. Systematic screening of LNA/2'-O-methyl chimeric derivatives of a TAR RNA aptamer. *FEBS Lett*. 2007;581(4):771–774.
46. Schmidt KS, Borkowski S, Kurreck J, et al. Application of locked nucleic acids to improve aptamer in vivo stability and targeting function. *Nucleic Acids Res*. 2004;32(19):5757–5765.
47. Hughesman CB, Turner RFB, Haynes CA. Measuring, intepreting and modeling the stabilities and melting temperatures of B-form DNAs that exhibit a two-state helix-to-coil transition. In: von Stockar U, van der Wielen LAM, editors. *Biothermondynamics: The Role of Thermodynamics in Biochemical Engineering*. Switzerland: EPFL Press, 2013:355–389.
48. Press WH, Flannery BP, Teukolsky SA, Vetterling WT. *Numerical Recipies in Fortran* (2nd edition). Cambridge University Press, 1992.
49. Hughesman C, Fakhfakh K, Bidshahri R, Haynes C. A new general model for predicting melting thermodynamics of complementary and mismatched duplexes containing locked nucleic acids: application to probe design for digital PCR detection of somatic mutations. *Biochemistry*. 2015;54(6):1338–1352.
50. Christensen U, Jacobsen N, Rajwanshi VK, Wengel J, Koch T. Stopped-flow kinetics of locked nucleic acid (LNA)-oligonucleotide duplex formation: studies of LNA-DNA and DNA-DNA interactions. *Biochem J*. 2001;354(Pt 3):481–484.
51. Di Giusto DA, King GC. Strong positional preference in the interaction of LNA oligonucleotides with DNA polymerase and proofreading exonuclease activities: implications for genotyping assays. *Nucleic Acids Res*. 2004;32(3):e32.
52. Hughesman CB, Turner RF, Haynes C. Stability and mismatch discrimination of DNA duplexes containing 2,6-diaminopurine and 2-thiothymidine locked nucleic acid bases. *Nucleic Acids Symp Ser (Oxf)*. 2008;(52):245–246.

Manuscript received Feb. 7, 2015, and revision received May 7, 2015.